TECHNICAL NOTES

NATIONAL ADVISORY COMMITTEE FOR AERONAUTICS

No. 831

A METHOD OF DETERMINING THE EQUILIBRIUM PERFORMANCE AND THE STABILITY OF AN ENGINE EQUIPPED WITH AN EXHAUST TURBOSUPERCHARGER

By James Buchanan Rea
Massachusetts Institute of Technology

Washington
November 1941

NATIONAL ADVISORY COMMITTEE FOR AERONAUTICS

TECHNICAL NOTE NO. 831

A METHOD OF DETERMINING THE EQUILIBRIUM PERFORMANCE AND THE STABILITY OF AN ENGINE EQUIPPED WITH AN EXHAUST TURBOSUPERCHARGER*

By James Buchanan Rea

SUMMARY

The performance of an exhaust turbine driving a supercharger is investigated by means of a sample calculation based on reasonable assumptions for the purpose of determining whether the assumed installation is stable with respect to changes in the mass of gas handled, boost pressure, etc. The arrangement was found to be stable throughout the entire range of operation. The method developed can be generally applied.

INTRODUCTION

This paper presents a method of determining the equilibrium performance and the stability of an engine equipped with an exhaust-turbine supercharger.

The exhaust-turbine supercharging mechanism is essentially composed of five parts: the engine, the nozzle box with nozzles, the turbine, the blower, and the intercooler. The sequence of events is shown schematically in figure 1.

The author wishes to express his appreciation to Professors C. Fayette Taylor and Edward S. Taylor for their guidance and supervision; and to Professor Joseph Keenan for his helpful suggestions.

---

*Thesis submitted in partial fulfillment of the requirements for the degrees of Bachelor of Science and Master of Science, Massachusetts Institute of Technology.

CHARACTERISTICS OF COMPONENTS

Symbols

The following list of symbols has been used in the analysis and charts of the present study.

W	weight
F/A	fuel-air ratio by weight
A	area
P	pressure
E	energy
H	total enthalpy
V	volume
v	specific volume
S	total entropy
T	absolute temperature (460 + ^{o}F)
E_s	internal energy
R	universal gas constant
U	velocity (speed)
g	acceleration of gravity
hp	horsepower
J	mechanical equivalent of heat
D	diameter
B	pressure coefficient
N	revolution speed, revolutions per minute
n	revolution speed, revolutions per second

c_p specific heat at constant pressure

c_v specific heat at constant volume

γ ratio of specific heats

I moment of inertia

η efficiency

ω angular velocity of rotating parts

$\dot{\omega}$ rate of change of angular velocity $(d\omega/dt)$

T torque

$Y_a = \left(\frac{P_i}{P_a}\right)^{0.2872} - 1$

r radius of blower to blade tip, feet

ρ density

Subscripts:

e exhaust gas (nozzle box)

i intake (before throttle)

N through nozzle

th throat

b blower

a air

w.g. waste gate

t turbine

ad adiabatic

av available

req required

Before the equilibrium performance of the complete supercharging operation can be determined, it is necessary to know the performance of each of the component parts of the supercharging mechanism.

The method of analysis will be illustrated by giving the analysis of a specific installation using the United States standard atmosphere as a basis for variations in atmospheric conditions with changes in altitude.

Engine Data

Assume the following test conditions:

(a) Wright G-102-A engine

(b) Engine speed held constant at 1900 rpm by propeller governor

(c) The temperature of the air entering the engine is that of the standard atmosphere corresponding to the entering pressure

(d) The engine will be run at full throttle

(e) Air consumption: 0.11 pound per brake-horsepower per minute

(f) Fuel/air ratio of 0.0782

In figure 2, the full-throttle brake horsepower is plotted against standard-density altitude for various engine speeds.

From figure 2 and reference 1, a curve of full-throttle brake horsepower against pressure before throttle was constructed and is given in figure 3. A curve of exhaust gas weight per second against brake horsepower is also plotted in figure 3.

Nozzle Data

Based upon the standard and accepted methods of nozzle design, the following fundamental nozzle data were used (critical conditions at nozzle throat):

(a) Simple converging nozzles of square cross section

(b) Total number of nozzles, 9

(c) Total nozzle throat area, 7.37 square inches

(d) Nozzle angle, 20°

The calculation of the nozzle performance curves will be treated in three parts:

(a) The effective ideal jet velocity.- It is assumed that the velocity of the gas as it hits the turbine wheel is the fully expanded velocity even though the velocity at the nozzle throat is not greater than the velocity of sound. This assumption, although not strictly correct for large changes in pressure across the nozzle, should be good in this analysis because of the comparatively large distance between the nozzle throat and the closest turbine blade. Above 30,000 feet this assumption should be used with caution because the higher the altitude the more the assumption is in error.

The velocity of the exhaust gas at the turbine blades can be calculated by the following formula:

$$U = \sqrt{\frac{\Delta H_e}{\left(1 + \frac{F}{A}\right)} 2g J} = 215.5 \sqrt{\Delta H_e} \qquad (1)$$

where

U velocity of exhaust gas hitting turbine blades, feet per second

ΔH_e change in enthalpy for $(1 + F/A)$ pounds of the exhaust gas as found from figure 4 by expanding adiabatically from the nozzle-box pressure and temperature to the atmosphere pressure outside the nozzle box

(Sufficiently accurate values of ΔH_e may be calculated from the perfect gas law provided that consistent values of γ, c_p, and R are used and that the correct value of R is also used. The data for figure 5 were calculated from equation (1) and from figure 4.)

(b) Weight rate of flow of exhaust gas through nozzles.- The weight rate of flow through the nozzles may be calculated by the following formula:

$$W_N = \frac{U_{th} A_{th}}{v_{th}} \left(1 + \frac{F}{A}\right) \qquad (2)$$

where

W_N weight rate of flow through nozzles, pounds per second

U_{th} velocity at nozzle throat, feet per second, calculated by using equation (1). In this case ΔH_e is the change in enthalpy obtained by merely expanding adiabatically to the throat pressure and not the atmospheric pressure

A_{th} throat area, total, square feet

v_{th} specific volume, found in figure 4 of $1 + \frac{F}{A}$ pounds of exhaust gas at the throat conditions

Results of calculations for W_N are plotted in figure 6.

(c) Nozzle horsepower.- The nozzle horsepower may be calculated by the following formula, where J is taken as 778 foot-pounds per Btu,

$$hp_N = W_N \frac{\Delta H_e \; 778}{\left(1 + \frac{F}{A}\right) 550} = 1.312 \; \Delta H_e \; W_N \qquad (3)$$

In this case, ΔH_e is the change in enthalpy for complete expansion of the exhaust gas to the pressure P_a because it is the horsepower of the exhaust gas as it contacts the turbine blades, which is the value desired. The results of the calculations are plotted in figure 7.

Turbine Data

A single-stage impulse turbine of 11.1 inches in diam-

eter was chosen. This turbine was assumed to have an efficiency curve as shown in figure 8, corresponding to a nozzle angle of 20°. This efficiency curve was taken from data in reference 3 (fig. 218, p. 234).

Blower Data

A single-stage, straight radial-blade, centrifugal blower 11.1 inches in diameter was used. The turbine and blower were directly connected. The details of the design of this blower have been omitted in this paper, but experimental curves for a blower of the same dimensions and design are given in figure 9.

Intercooler Data

It will be assumed that an intercooler is provided and regulated so that the temperature of the air entering the engine is the standard United States atmospheric temperature (reference 1), corresponding to the pressure of the entering air. The pressure drop of the charge air has been neglected but, in general, as pointed out in reference 4, it should be taken into account.

DETERMINATION OF EQUILIBRIUM PERFORMANCE

Now that the performance curves for each component part of the supercharging mechanism have been determined, the over-all performance will be obtained for the equilibrium conditions.

First, curves of required pressure coefficient against revolution speed at various altitudes and for various full-throttle brake horsepowers are determined by the use of the following equation, which involves the definition of B, the pressure coefficient.

$$B \frac{U_b^2}{g} = J c_{p_a} T_a Y_a \qquad (4)$$

where the significance of the subscripts and the units used in the calculations are as follows:

U_b tip speed of the blower, feet per second

T_a outside-air temperature, °F absolute

$$Y_a = \left(\frac{P_i}{P_a}\right)^{\frac{\gamma_a - 1}{\gamma_a}} - 1$$

P_i intake manifold pressure, pounds per square inch

P_a standard atmospheric pressure, pounds per square inch

γ_a ratio of specific heats c_{p_a}/c_{v_a}; for air $(\gamma_a - 1)/\gamma_a = 0.2872$

D_b blower diameter, feet

N_b revolution speed of blower, revolutions per minute

Thus

$$B = \frac{J\, c_{p_a}\, T_a \left[\left(\frac{P_i}{P_a}\right)^{0.2872} - 1\right] g}{\left(\frac{\pi\, D_b\, N_b}{60}\right)^2}$$

But

$$\frac{J\, c_{p_a}\, g}{\left(\frac{\pi\, D_b}{60}\right)^2} = \frac{(778)\ (0.2397)\ (32.2)\ (3600)}{(3.142)^2\ \left(\frac{11.1}{12}\right)^2} = 25.6 \times 10^5$$

so

$$B = 25.6 \times 10^5\, \frac{T_a\, Y_a}{N_b^2}$$

or

$$B = 2.56\, \frac{T_a\, Y_a}{\left(\frac{N_b}{1000}\right)^2} \qquad (5)$$

A curve of Y_a for various values of P_i/P_a is given in figure 10. The required pressure coefficients have been computed and the results are plotted as solid-line curves in figure 11.

Second, curves of available pressure coefficient against blower speed, at various altitudes and for various full-throttle brake horsepowers are determined from the formula

$$V_{req} = v_a \, c \, \frac{A}{F} \, bhp \qquad (6)$$

where v_a is specific volume and c is specific fuel consumption. At a given altitude and brake horsepower, values of $\frac{V_{req}}{N_b \, D_b^3}$ can be calculated from equation (6) for various values of N_b. From figure 9 values of available pressure coefficients corresponding to values of $\frac{V_{req}}{N_b \, D_b^3}$ are determined. The calculated available pressure coefficients are plotted as dotted-line curves in figure 11.

The intersection of corresponding curves of available and required pressure coefficients gives data for curves of blower speed required against altitude for various brake horsepowers. Since the blower and the turbine are directly connected, it is possible to calculate curves of turbine tip speed required against altitude for various brake horsepowers. These curves are shown in figure 12; the following formula was used as the basis of calculation:

$$\text{Turbo. tip-speed} = \left(\frac{\pi}{60}\right)(D_t) \, N_{b_{req}} = 0.04842 \, N_{b_{req}} \qquad (7)$$

Third, blower shaft horsepower required against altitude was determined for various brake horsepowers as follows: Since values of required blower speeds against altitude at various brake horsepowers are known and since values of V_{req} against altitude at various brake horsepowers can be found from equation (6), it follows that values of $\frac{V_{req}}{N_{req} \, D_b^3}$ can be calculated for different altitudes and at various brake horsepowers. Thus, from figure 9, values of adiabatic efficiency η_{ad} can be determined for corresponding values of $\frac{V_{req}}{N_{req} \, D_b^3}$. The value of η_{ad} used was taken

from figure 9(a) or 9(b) depending on which rpm range more closely corresponded to the rpm used in the example. It is assumed here that η_{ad} is a function only of $\frac{V_{req}}{N_{req} D_b^3}$ and is independent of N_{req}, which is very nearly true as can be seen from figure 9. Values of required adiabatic horsepower for various altitudes and engine brake horsepowers are easily calculated by the formula below:

$$(hp_{ad})_{req} = \frac{J\, c_{p_a}\, W_i\, T_a\, Y_a}{33000} = 0.0006215\ (bhp)\ (T_a\, Y_a) \qquad (8)$$

where W_i is the air consumption, pounds per minute.

Finally, corresponding values of adiabatic efficiency and adiabatic horsepower required being known, curves of blower-shaft horsepower required against altitude, for various brake horsepowers, may be plotted as shown in figure 13, using the following relation:

$$\text{Blower-shaft } hp_{req} = \frac{\text{adiabatic } hp_{req}}{\eta_{ad}} \qquad (9)$$

Fourth, curves of nozzle-box pressure required against altitude are determined for various brake horsepowers by the use of figures 5, 7, 8, 12, and 13, as follows: Decide upon a constant brake horsepower. An altitude should then be chosen and the turbine tip speed required obtained from figure 12. A value of the required nozzle-box pressure should be chosen and the nozzle gas velocity and the nozzle horsepower at the assumed altitude should be obtained from figures 5 and 7, respectively. With the nozzle velocity and the required turbine tip speed, the turbine adiabatic efficiency may be obtained from figure 8. Then the blower-shaft horsepower is obtained by multiplying the efficiency by the nozzle horsepower. With this blower-shaft horsepower, an altitude is obtained from figure 13 at the constant brake horsepower first decided upon. If this altitude does not agree with the altitude chosen at the beginning, then a different value of the required nozzle-box pressure is taken and successive efforts are made until the sequence is in consistent equilibrium.

This process may seem very long and tedious, but experience has shown that the equilibrium value of the turbine

efficiency varies by only a slight amount with changes in altitude at constant brake horsepower. Thus, the number of trials necessary is seldom more than two if a turbine efficiency is first estimated and later substantiated by using the foregoing curves.

Figure 14 shows the results of the foregoing method.

From figures 14 and 6, curves of required nozzle weight rate of flow against altitude for various brake horsepowers may be determined; they are shown in figure 15.

Fifth, curves of required "nozzle-equivalent" waste-gate area against altitude are determined for various brake horsepowers, as follows: At any given altitude, the weight rate required through the nozzles in order to maintain a given brake horsepower is found from figure 15. The exhaust-gas weight rate available is determined from figure 3, and the difference between these two rates represents the weight rate that must pass through the waste gate. Now, since the pressure required and the assumed constant temperature of the gas in the nozzle box are known, figure 4 may be used to find the change in enthalpy of the gas leaving the nozzle box. Also, figure 4 may be used to find v, the chart volume of the gas as it leaves the waste gate. These values being known, the required "nozzle-equivalent" waste-gate area may be found by the condition of continuity, as represented by the following equation:

$$A_{w.g.} = \frac{W_{exhaust}\, v}{\sqrt{\Delta H_e}\ \sqrt{778 \times 2g\left(1 + \frac{F}{A}\right)}} \qquad (10)$$

A much simpler method of calculating the "nozzle equivalent" waste-gate area is shown in the following equation:

$$A_{w.g.} = A_N \frac{W_{exhaust}}{W_{req}} \qquad (11)$$

Figure 16 shows the curves resulting from equation (12) for required "nozzle-equivalent" waste-gate area against altitude, at various brake horsepowers.

Discussion

The curves of required pressure shown in figure 14 indicate a definite minimum. This fact is substantiated by experimental curves of Berger and Chenoweth (reference 4), reproduced in figure 17.

It should be remembered that the analysis thus far is only valid for determining the equilibrium conditions of the supercharging cycle. But once these conditions have been determined, the static and the dynamic stability of the system may be easily found by assuming a small change in one of the variables and following this effect completely through the cycle. Equilibrium conditions cannot occur at altitudes above that at which the curve of weight rate required is intersected by the curve of weight rate available, for constant brake horsepower. (See fig. 15.) In this particular example, these curves do not intersect within the ranges investigated, but they might intersect if experimental data rather than theoretically calculated data, were used throughout the analysis.

It is possible for the system to be in equilibrium even though it is statically unstable. In other words, a slight change in one of the variables from its equilibrium value might not be followed by a tendency for the system to return to its original state. It may also be possible for the system to be statically stable but dynamically unstable, that is, a slight change in one of the variables from its equilibrium value might result in an undamped and cumulating oscillation.

DETERMINATION OF STATIC STABILITY

Development of Formulas Used in Static-Stability Calculations

The fundamental expression used in determining the stability of the exhaust-turbine supercharging cycle is based upon Newton's second law of motion, and is as follows:

$$\frac{d\,(T_t - T_b)}{d\omega} < 0 \qquad (12)$$

where

ω angular velocity of rotating parts, radians/second

T_t turbine torque, foot-pounds

T_b blower torque, foot-pounds

An expression for the turbine torque T_t is derived from the basic equation for horsepower:

$$\text{Turbine hp} = \frac{T_t \omega}{550} \tag{13}$$

also

$$\text{Turbine hp} = hp_N \eta_t \tag{14}$$

where

hp_N horsepower of exhaust gas from nozzles as it comes in contact with turbine blades

η_t turbine efficiency (See fig. 8.)

If equations (13) and (14) are combined, there is obtained for turbine torque

$$T_t = \frac{hp_N \ \eta_t \ 550}{\omega} \tag{15}$$

An expression for the blower torque may also be found by using the basic equation for horsepower:

$$\text{Blower-shaft hp} = \frac{T_b \omega}{550} \tag{16}$$

also,

$$\eta_b = \frac{\text{Adiabatic hp}}{\text{Blower-shaft hp}} \tag{17}$$

where η_b is the adiabatic efficiency of the blower and is defined by equation (17). The adiabatic horsepower can be obtained from equation (8).

$$\text{Adiabatic hp} = \frac{J \ c_{p_a} \ W_i \ T_a \ Y_a}{33000}$$

By the introduction of equation (4) and the equality $U_b = \omega r$, an expression may be developed as follows:

$$B\omega^2 = \frac{g \ J \ c_{p_a} \ T_a \ Y_a}{r^2} \tag{18}$$

Equations (16), (17), and (18) may be combined to give a final expression for the blower torque,

$$T_b = \left(\frac{B}{\eta_b}\right) \omega r^2 \left(\frac{W_i}{60\ g}\right) \tag{19}$$

Additional equations, such as

$$W_i = (\text{bhp})\ (0.11) \tag{20}$$

are needed for the stability calculations.

Since $N_b = \frac{60\,\omega}{2\pi}$ and since $W_i = V\,\rho_a$, an expression for the dimensionless blower coefficient $\frac{V}{N_b D_b^3}$ is easily developed:

$$\frac{V}{N_b\ D_b^3} = \left(\frac{W_i}{\omega}\right)\left(\frac{2\pi}{60\ \rho_a\ D_b^3}\right) \tag{21}$$

also

$$W_e = W_N + W_{exhaust} \tag{22}$$

and

$$W_{exhaust} = W_N\left(\frac{A_{w.g.}}{A}\right) \tag{23}$$

thus,

$$W_N = \left(\frac{W_e}{1 + \frac{A_{w.g.}}{A_N}}\right) \tag{24}$$

Procedure for Determining Static Stability

Select an altitude at which the stability is to be investigated. This altitude will determine the pressure, the temperature, and the density of the air as consistent with the standard atmosphere. Columns 22, 23, 24, and 25 of table I may be filled in immediately. Then, decide upon an equilibrium value of the brake horsepower (column 1) at this altitude and from the equilibrium-performance calculations, determine the corresponding value of the waste-gate area (nozzle equivalent) for column 13. The value of W_e (column 2) may be found from figure 3; P_i (column 3) may be found by using figure 3; and W_i (column 4) may be found by using equation (20). Column 5 = $\frac{\text{column 3}}{\text{column 23}}$; Column 6 is

obtained by using column 5 and figure 10. Column 7 may be found using equation (18).

Next, estimate a value of ω and use equation (21) to get $\frac{V}{N_b D_b^3}$. Then, get the corresponding value of B from figure 9 and calculate $B\omega^2$. When this value agrees with the value in column 7, the ω is correct, and the η_b may then be determined from figure 9 corresponding to the correct value of $\frac{V}{N_b D_b^3}$. Thus, columns 8, 9, 10, and 11 may be filled in once this equilibrium value of ω has been obtained. Column 12 may be calculated using equation (19). Column 13 is determined from the equilibrium-performance calculations, and column 14 may therefore be obtained from equation (24). With the value in column 14 enter figure 6 at the proper altitude and get P_e for column 15. Then, with this value of P_e, get hp_N (column 16) from figure 7 at the correct altitude. Also get U_g (column 17) from figure 5, using the foregoing value of P_e and the same altitude. Column 18 = $\frac{\text{column 8 r}}{\text{column 17}}$, and this value may be used to obtain η_t (column 19) from figure 8. Now, T_t (column 20) may be calculated using equation (15). Column 21 is found by subtracting column 12 from column 20.

Finally, a plot of $I\dot{\omega}$ against ω may be made as shown in figure 18. Each line in this figure represents the stability at a constant altitude, for a fixed waste-gate position and for the equilibrium horsepower corresponding to this fixed waste-gate position. The system is stable for any altitude and waste-gate position only when the slope of the corresponding line is negative, that is, a decrease in ω from its equilibrium value causes an increase in $T_t - T_b$, thus causing the system to return to its equilibrium conditions. On the other hand, an increase in ω would cause a decrease in $T_t - T_b$ for a stable system.

Figure 18 seems to indicate that, for a constant value of the equilibrium horsepower, the stability decreases with increase in altitude as shown by the 600-horsepower curves at 20,000 and 25,000 feet. An increase in horsepower at the same altitude seems to affect the stability very little.

DISCUSSION

It should be remembered that the shape of the actual curves as obtained by the equilibrium performance and the stability calculations made in this analysis depend upon the original characteristics of each component part of the supercharging cycle. The analysis of a particular theoretically calculated cycle was made in this case merely to outline a general procedure that could be used in determining the over-all characteristics and stability of any exhaust turbine supercharger installation.

Turbosupercharger installations are apparently statically unstable in the region of low V/nD^3 where the supercharger stalls and the curve of B (or q) plotted against V/nD^3 is discontinuous. Dynamic instability is frequent but is caused principally by control difficulties, and consideration of it has therefore been avoided in this paper.

It is generally known that in the past many actual exhaust-turbine installations have been unstable under certain critical conditions. Because of the secrecy at the present time in connection with the general subject of exhaust turbines, the author has found it impossible to obtain data necessary for an analysis of any actual installation.

It is suggested that, if an analysis of this type were made prior to the installing of any exhaust-turbine system, information might be discovered which would help to eliminate causes for unstability and thus enable the designer to obtain a reasonable estimate of the performance of the entire supercharging cycle.

Massachusetts Institute of Technology,
Cambridge, Mass., May 15, 1941.

REFERENCES

1. Brombacher, W. G.: Altitude-Pressure Tables Based on the United States Standard Atmosphere. Rep. No. 538, NACA, 1935.

2. Hershey, R. L., Eberhardt, J. E., and Hottel, H. C.: Thermodynamic Properties of the Working Fluid in Internal-Combustion Engines. SAE Jour., vol. 39, no. 4, Oct. 1936, pp. 409-424.

3. Stodola, A.: Steam and Gas Turbines, pt. I. McGraw-Hill Book Co., Inc., 1927.

4. Berger, A. L., and Chenoweth, Opie: Supercharger Installation Problems. SAE Jour., vol. 43, no. 5, Nov. 1938, pp. 472-484.

TABLE I - COMPUTATION OF STABILITY

$B\omega^2 = \frac{gJc_{p_a}T_aY_a}{r^2}$; $\frac{V}{N_bD_b^3} = \left(\frac{W_1}{\omega}\right)\left(\frac{2\pi}{60\rho_aD_b^3}\right)$; $W_1 = 0.11bhp$; $T_b = \left(\frac{B}{\eta_b}\right)\omega r^2\left(\frac{W_1}{60g}\right)$; $W_N = \frac{W_e}{1 + \frac{A_{w.s.}}{A_N}}$; $I\dot{\omega} = T_t - T_b$;

$T_t = \frac{550\ hp_N\eta_t}{\omega}$; $A_N = 0.0512$ sq ft; F/A = 0.0872; $D_b^3 = 0.792$ cu ft; g = 32.2 ft/sec/sec; J = 778; $c_{p_a} = 0.239T$; r = 0.4625

(22) Altitude (ft)	(23) P_a (in. Hg)	(24) T_a (°F abs)	(25) ρ_a ($\frac{lb}{cu\ ft}$)	(3) P_i (in. Hg)	(4) W_i ($\frac{lb}{min}$)	(5) $\frac{P_i}{P_a}$	(6) Y_a	(7) $B\omega^2$	(8) ω (radians/sec)	(9) $\frac{V}{ND^3}$	(10) B
600 hp equilibrium											
20,000	13.74	447.1	0.04100	18.95	66.0	1.379	0.092	11.54 x 10^5	1405	0.1513	0.590
				25.	85.8	1.819	.186	23.32	1925	.1456	.625
				15.8	55.0	1.150	.036	4.52	975	.1818	.477
25,000	11.10	429.2	0.03940	18.95	66.0	1.706	0.162	19.49	1750	0.1281	0.650
				25.	85.8	2.252	.261	31.42	2205	.1303	.647
				15.8	55.0	1.423	.102	12.27	1385	.1332	.638
30,000	8.88	411.4	0.02863	18.95	66.0	2.133	0.242	27.92	2115	0.1459	0.624
				25.	85.8	2.817	.346	39.92	2580	.1535	.598
				12.	41.25	1.351	.086	9.915	1285	.1482	.599
35,000	7.04	393.6	0.02371	18.95	66.0	2.692	0.329	36.25	2445	0.1504	0.608
				25.	85.8	3.552	.440	48.60	2935	.1628	.565
				12.	41.25	1.704	.162	17.88	1680	.1369	.630

(22) Altitude (ft)	(11) η_b	(12) T_b (ft-lb)	(13) $A_{w.s.}$ (sq ft)	(14) W_N ($\frac{lb}{sec}$)	(15) P_e ($\frac{lb}{sq\ in.}$)	(16) hp_N	(17) Ug ($\frac{ft}{sec}$)	(18) $\frac{\omega r}{Ug}$	(19) η_t	(20) T_t (ft-lb)	(21) $I\dot{\omega}$ (ft-lb)	(2) W_e ($\frac{lb}{sec}$)	(1) bhp
600 hp equilibrium													
20,000	0.655	9.26	0.0443	0.635	8.9	53	1340	0.485	0.742	9.59	0.33	1.185	600
	.669	17.09	.0443	.826	10.3	61	1620	.550	.727	12.67	-4.42	1.540	780
	.560	5.09	.0443	.529	8.2	21	1130	.399	.712	8.45	3.36	.988	500
25,000	0.694	11.85	0.0361	0.695	8.45	52	1620	0.494	0.742	12.28	0.43	1.185	600
	.682	19.89	.0361	.903	10.85	105	2040	.501	.741	19.40	- .49	1.540	780
	.688	7.83	.0361	.579	7.40	31	1350	.475	.741	9.12	1.29	.988	500
30,000	0.669	14.42	0.0354	0.701	8.4	75	1950	0.502	0.742	14.48	0.06	1.185	600
	.650	22.56	.0354	.911	10.8	133	2290	.521	.738	20.91	-1.65	1.540	780
	.662	5.32	.0354	.438	6.05	23	1370	.434	.731	7.19	1.87	.741	375
35,000	0.657	16.55	0.0361	0.695	8.3	100	2280	0.497	0.742	16.68	0.13	1.185	600
	.621	25.37	.0361	.903	10.8	166	2570	.528	.736	22.90	-2.47	1.540	780
	.683	7.08	.0361	.435	5.55	35	1650	.472	.741	8.50	1.42	.741	375

(22) Altitude (ft)	(23) P_a (in. Hg)	(24) T_a (°F abs)	(25) ρ_a ($\frac{lb}{cu\ ft}$)	(3) P_i (in. Hg)	(4) W_i ($\frac{lb}{min}$)	(5) $\frac{P_i}{P_a}$	(6) Y_a	(7) $B\omega^2$	(8) ω (radians/sec)	(9) $\frac{V}{ND^3}$	(10) B
925 hp equilibrium											
15,000	16.88	464.9	0.04820	29.92	101.8	1.772	0.175	22.82 x 10^5	1932	0.1444	0.623
				20.	69.5	1.186	.049	6.39	1110	.1716	.518
				25.	85.8	1.481	.117	15.26	1595	.1474	.601
				31.25	106.2	1.851	.191	24.91	2003	.1454	.621
25,000	11.10	429.2	0.03940	29.92	101.8	2.695	0.329	39.62	2494	0.1369	0.636
				20.	69.5	1.801	.183	21.98	1841	.1266	.651
				31.25	106.2	2.815	.348	41.90	2570	.1386	.634
				25.	85.8	2.252	.262	31.55	2210	.1301	.647
20,000	13.74	447.1	0.04100	29.92	101.8	2.177	0.250	31.32	2250	0.1458	0.619
				20.	69.5	1.455	.110	13.78	1515	.1477	.601
				25.	85.8	1.818	.186	23.30	1930	.1432	.625
				31.25	106.2	2.275	.266	33.32	2325	.1472	.617
30,000	8.88	411.4	0.02863	29.92	101.8	3.370	0.418	48.22	2910	0.1614	0.570
				20.	69.5	2.252	.261	30.11	2205	.1454	.621
				25.	85.8	2.817	.346	39.92	2580	.1534	.598
				31.25	106.2	3.521	.436	50.30	2995	.1637	.562

(22) Altitude (ft)	(11) η_b	(12) T_b (ft-lb)	(13) $A_{w.s.}$ (sq ft)	(14) W_N ($\frac{lb}{sec}$)	(15) P_e ($\frac{lb}{sq\ in.}$)	(16) hp_N	(17) Ug ($\frac{ft}{sec}$)	(18) $\frac{\omega r}{Ug}$	(19) η_t	(20) T_t (ft-lb)	(21) $I\dot{\omega}$ (ft-lb)	(2) W_e ($\frac{lb}{sec}$)	(1) bhp
925 hp equilibrium													
15,000	0.668	20.30	0.0332	1.110	13.7	95	1755	0.510	0.740	20.02	-0.28	1.827	925
	.596	7.43	.0332	.757	10.5	32	1250	.411	.722	11.46	4.03	1.248	632
	.664	13.70	.0332	.934	11.9	58	1500	.492	.742	14.85	1.15	1.540	780
	.666	21.98	.0332	1.157	14.15	106	1800	.515	.738	21.46	- .52	1.906	966
25,000	0.677	26.43	0.0310	1.140	13.6	169	2310	0.500	0.742	27.68	1.25	1.827	925
	.683	13.51	.0310	.778	9.4	77	1820	.468	.741	16.79	3.28	1.248	632
	.676	28.34	.0310	1.187	14.15	183	2360	.504	.741	29.00	.66	1.906	966
	.682	19.90	.0310	.959	11.4	118	2100	.487	.743	21.80	1.90	1.540	780
20,000	0.666	23.58	0.0323	1.120	13.4	130	2020	0.516	0.738	23.45	-0.13	1.827	925
	.664	10.55	.0323	.765	9.8	50	1530	.458	.740	13.43	2.88	1.248	632
	.669	17.14	.0323	.944	11.5	86	1800	.496	.742	18.18	1.04	1.540	780
	.664	25.42	.0323	1.169	13.9	141	2060	.522	.737	24.58	- .84	1.906	966
30,000	0.625	29.92	0.0289	1.170	13.9	213	2570	0.524	0.737	29.69	-0.23	1.827	925
	.666	15.85	.0289	.798	9.6	102	2130	.479	.742	18.86	3.01	1.248	632
	.650	22.54	.0289	.984	11.8	157	2380	.501	.742	24.84	2.30	1.540	780
	.618	32.05	.0289	1.218	14.5	230	2610	.551	.734	31.02	-1.03	1.906	966

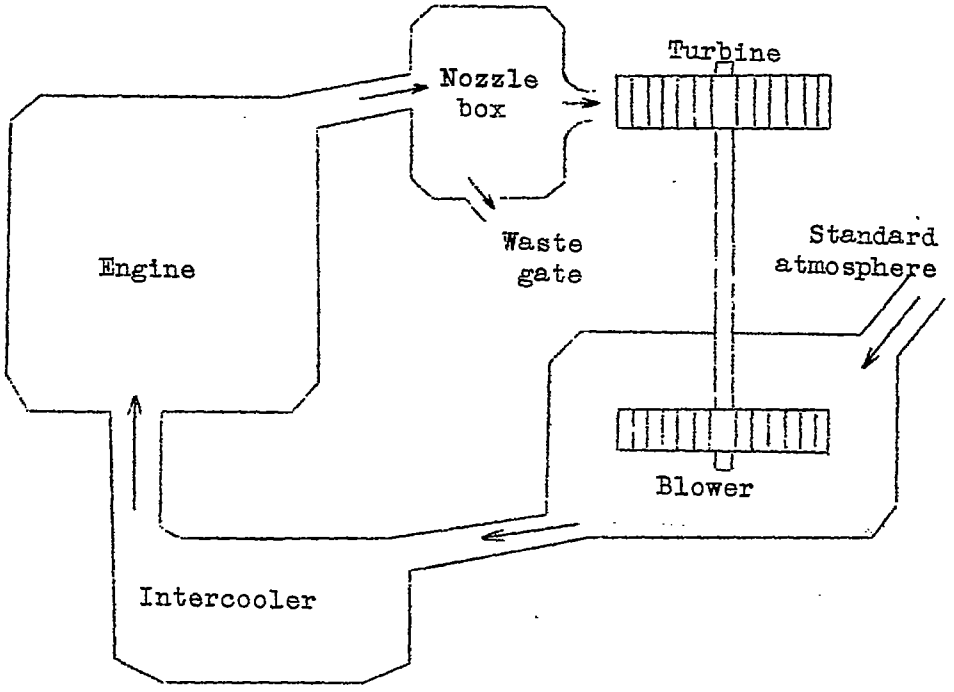

Figure 1.- Schematic sketch of the exhaust-turbine supercharging mechanism.

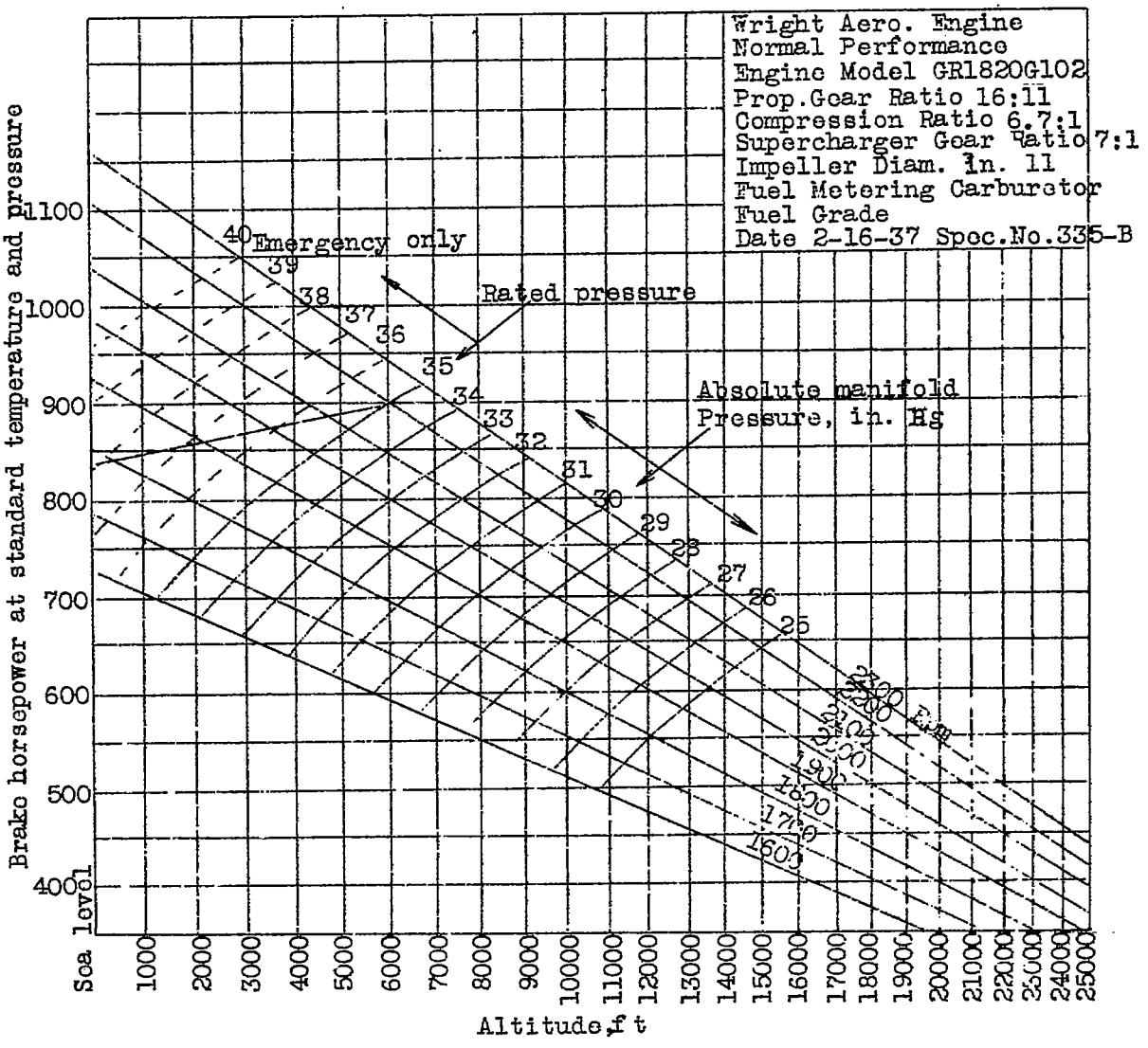

Figure 2.- Altitude performance. Horsepower and manifold pressure (without ram) for Wright G-102-A aircraft engine. (From book of instructions on Wright Cyclone Engine, GR-1820-G100.)

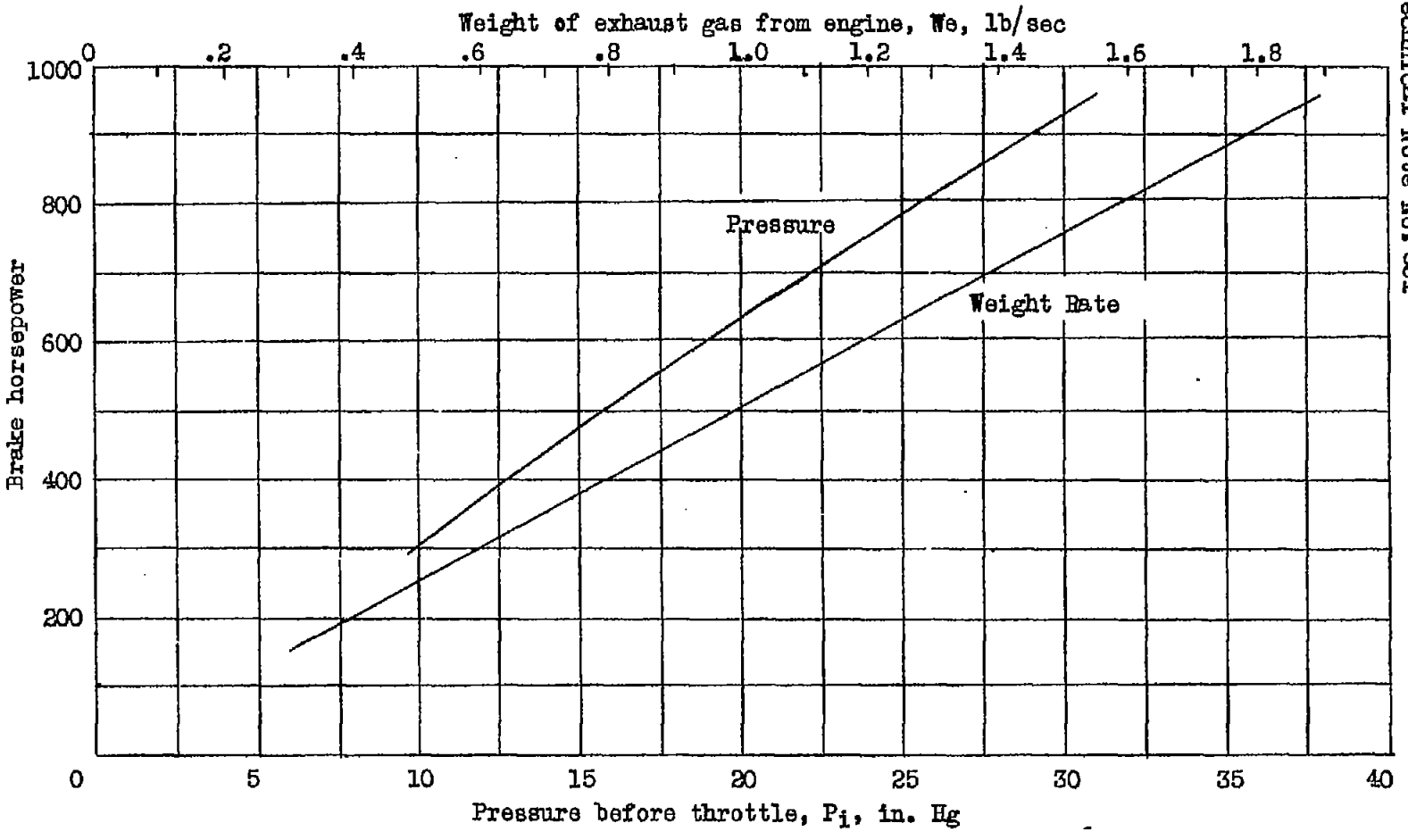

Figure 3.- Variation of exhaust-gas weight and pressure before throttle with brake horsepower, Wright G-120-A engine; engine speed, 1900 rpm; full throttle; fuel-air ratio, 0.0782.

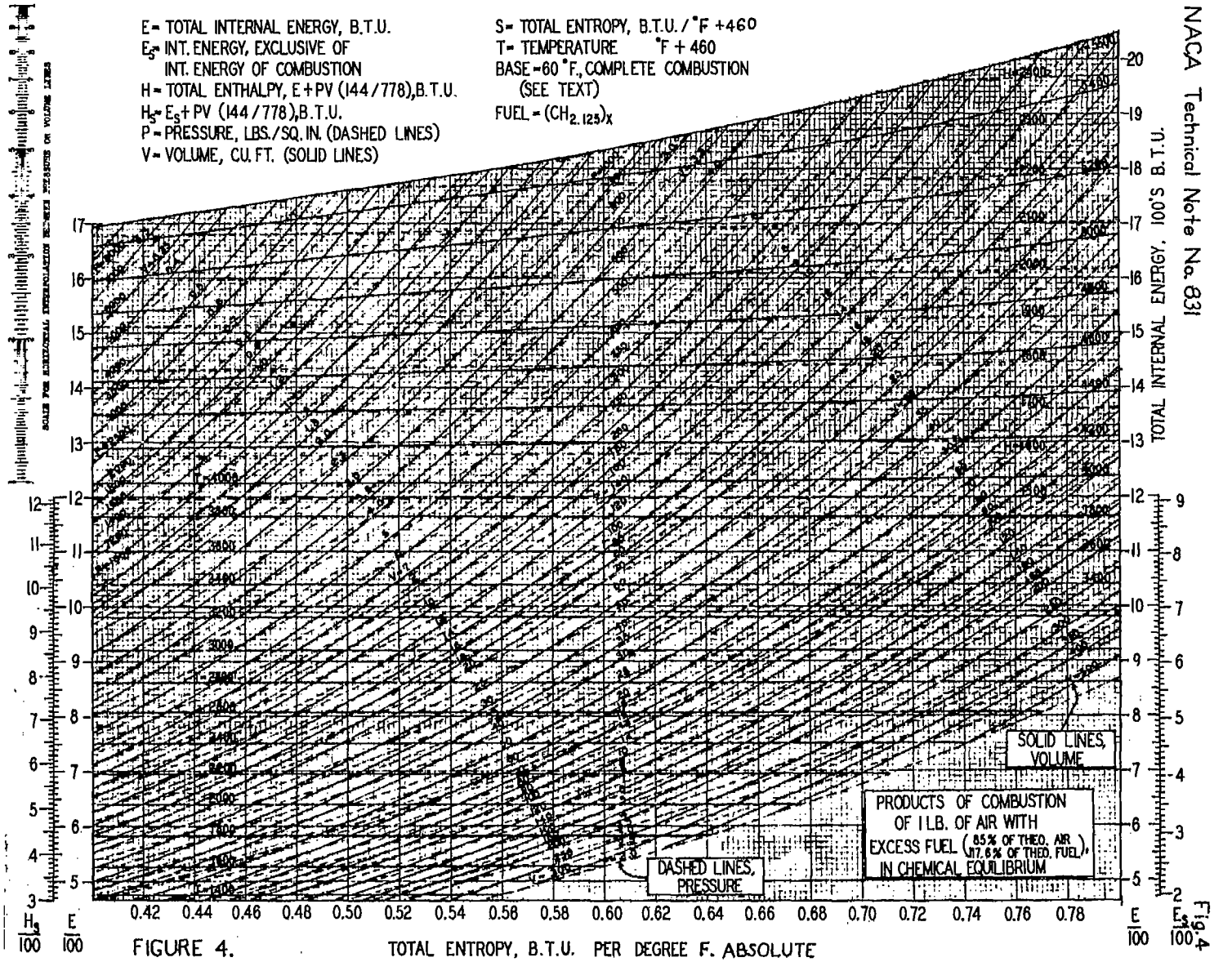

FIGURE 4.

Fig. 4

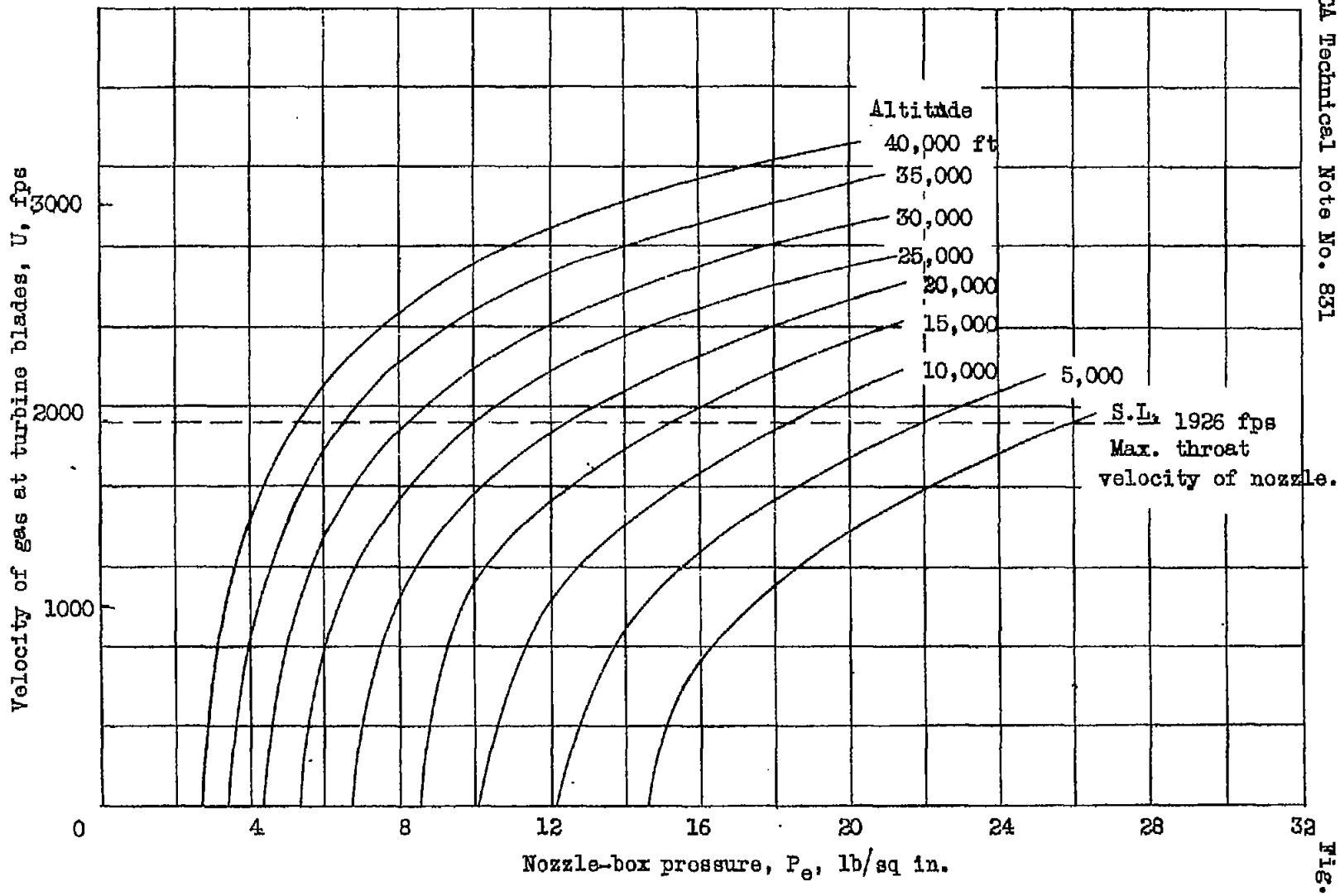

Fig. 5

Figure 5.- Variation of velocity of gas at turbine blades with nozzle-box pressure.

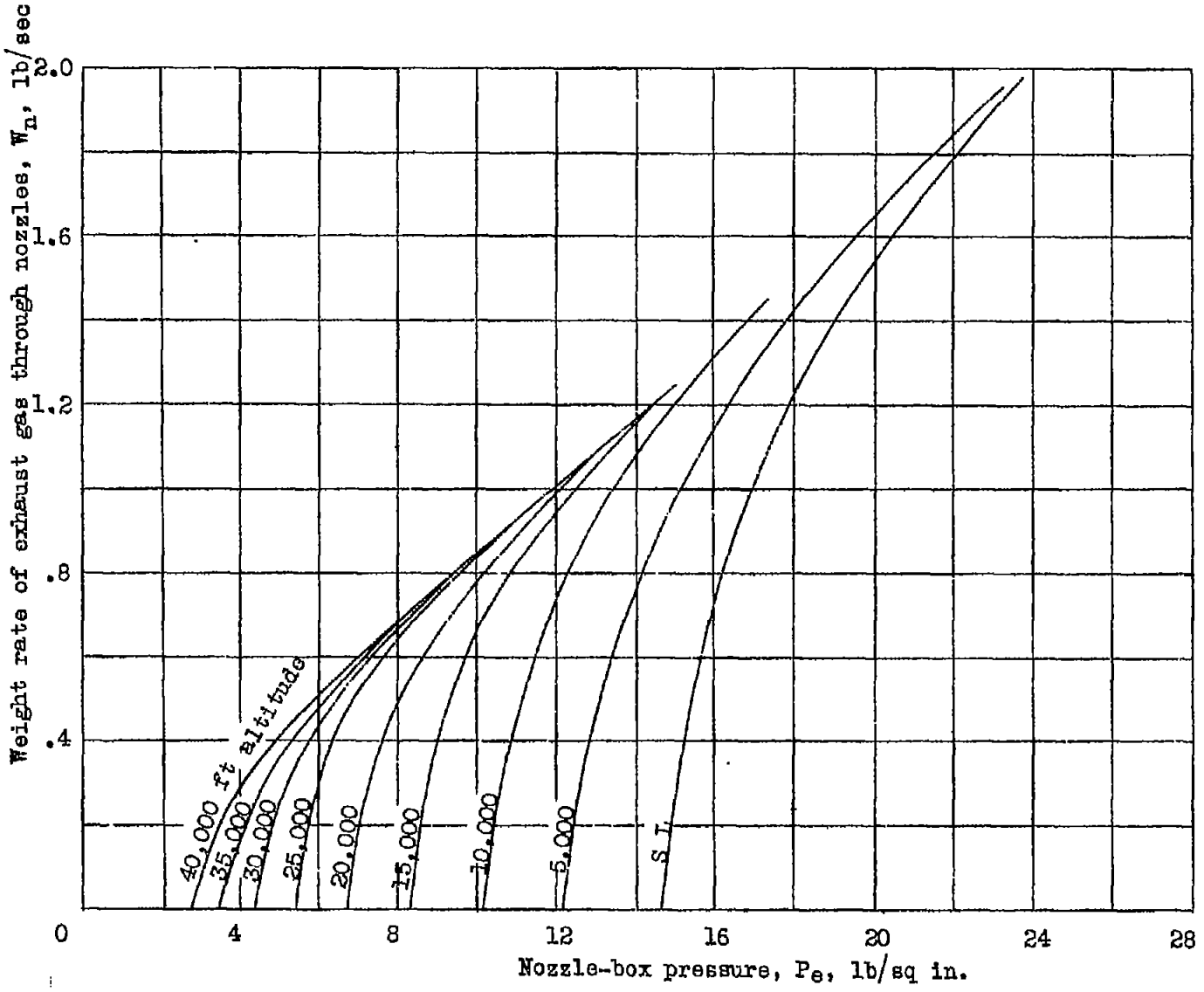

Figure 6.- Variation of weight rate of exhaust gas through nozzle with nozzle-box pressure.

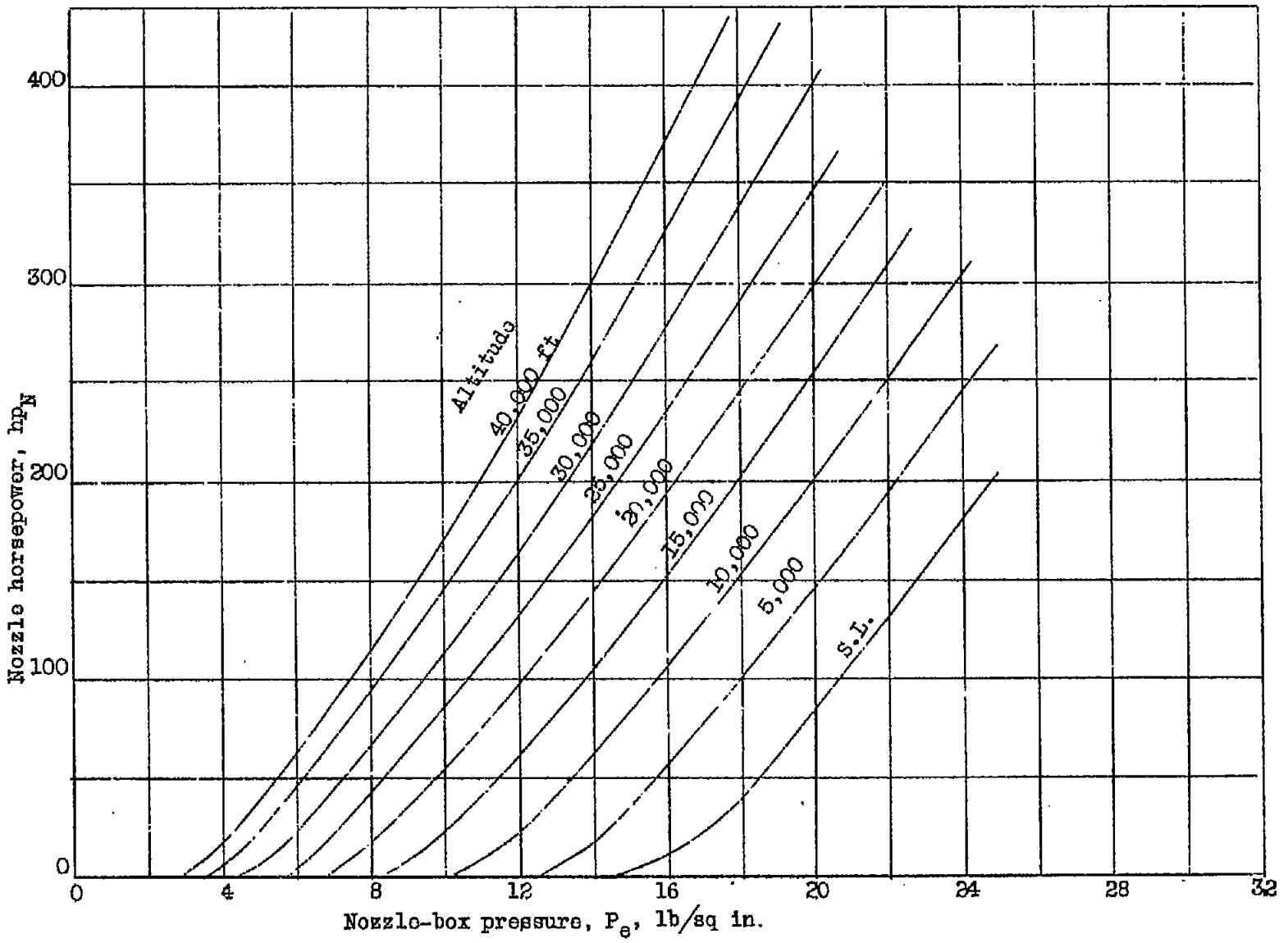

Figure 7.

Figure 7.-Variation of nozzle-horsepower with nozzle-box pressure.

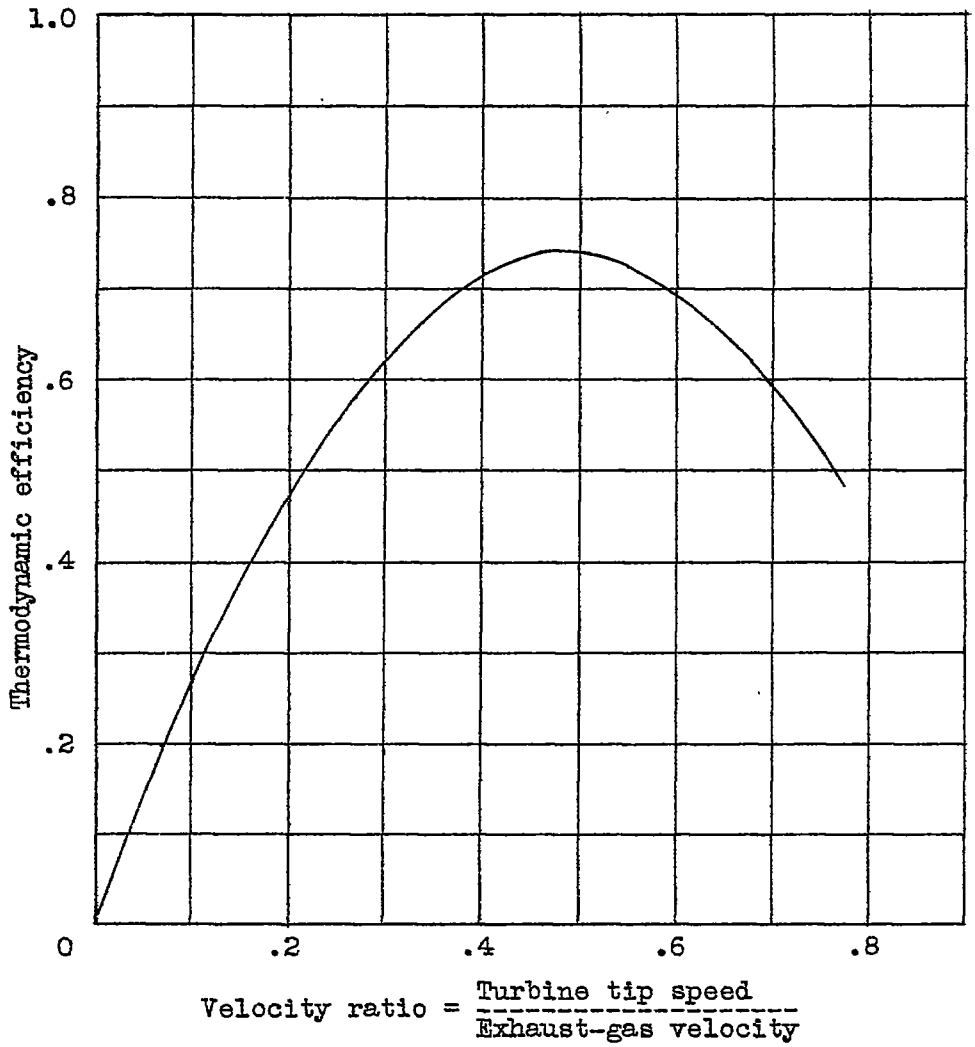

Figure 8.- Variation of efficiency with velocity ratio for single-stage impulse turbine with nozzle angle of 20° (from reference 3).

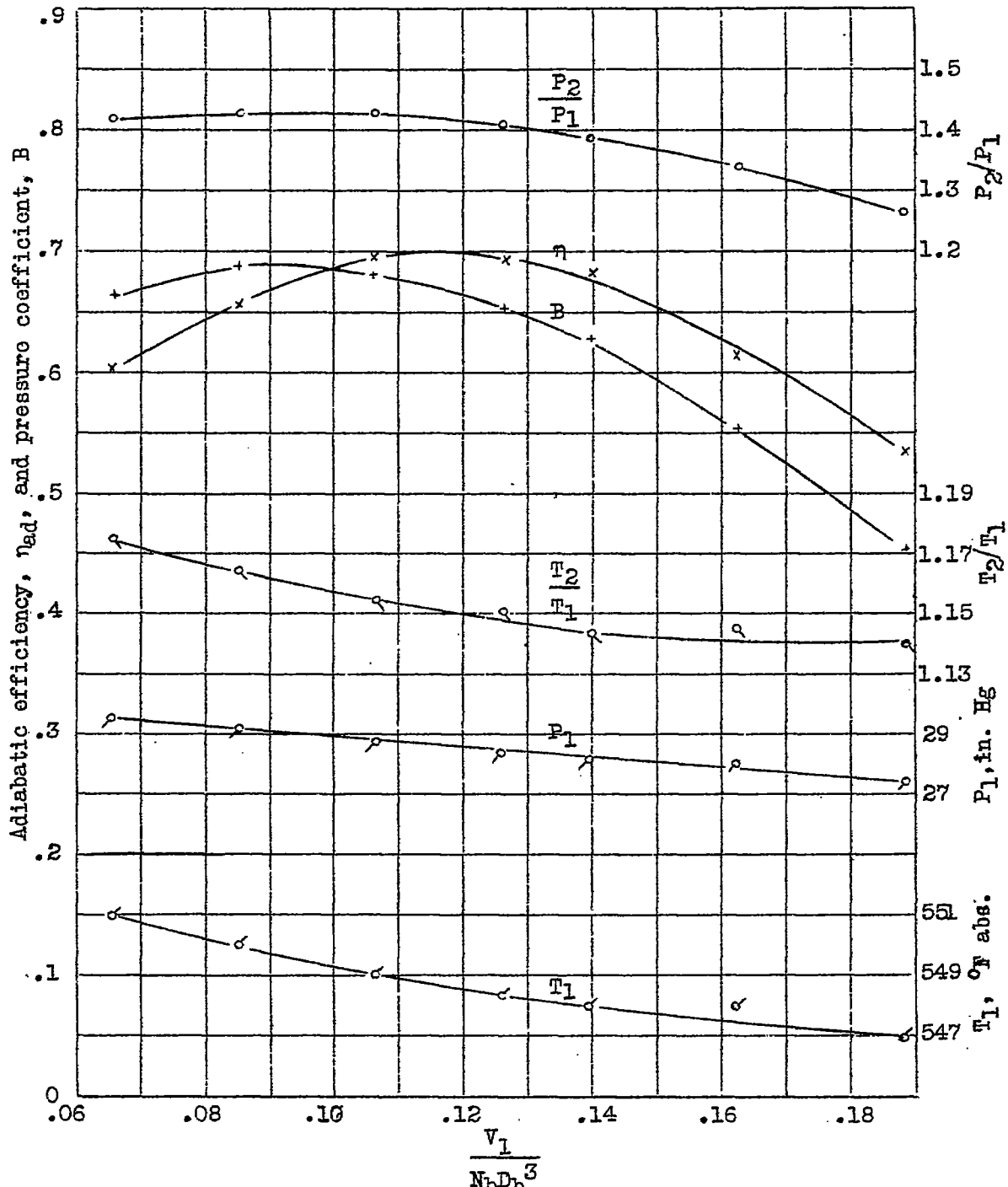

Figure 9a.- Characteristics of Cyclone supercharger at 15,000 rpm; tip speed, 720 fps.

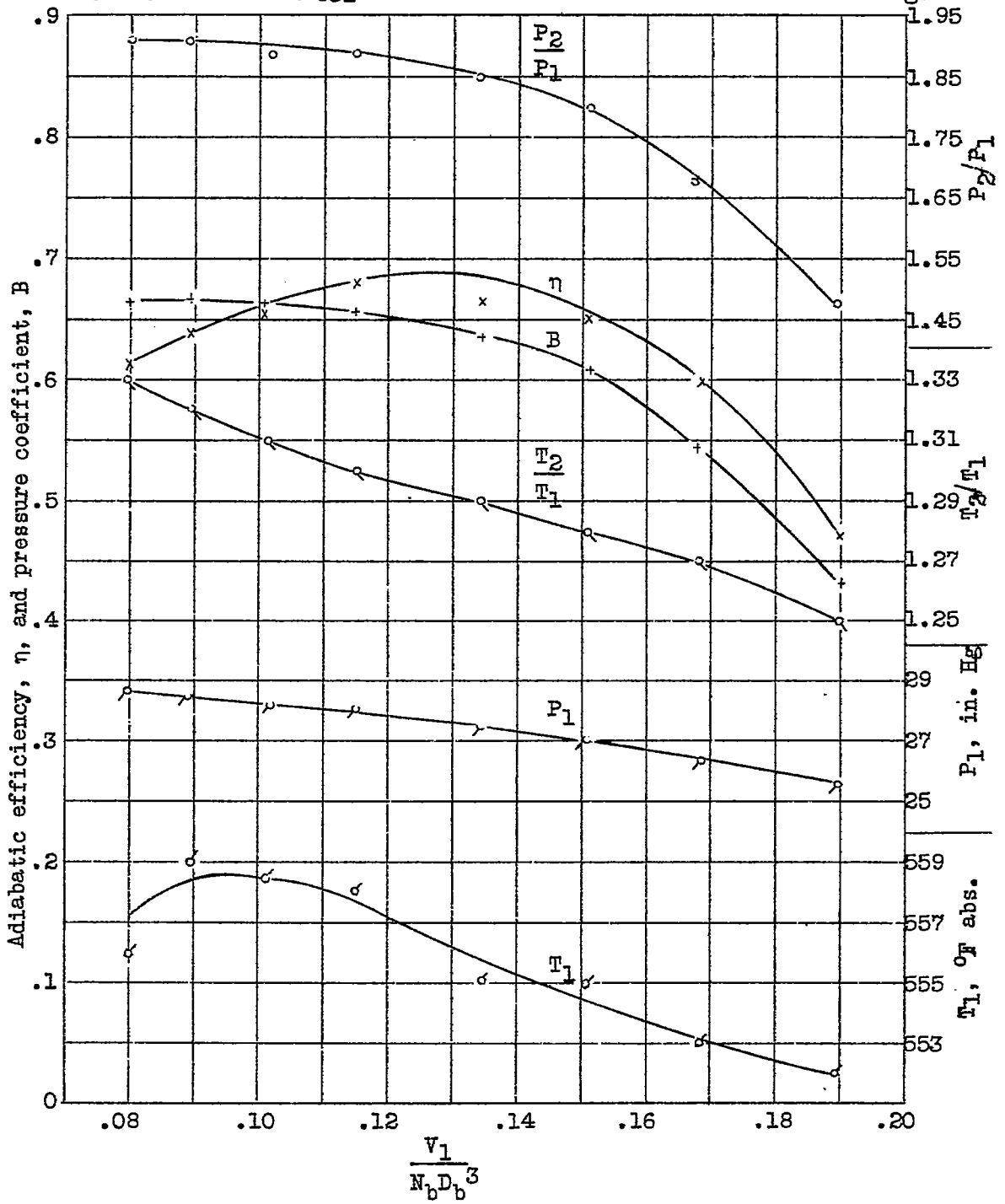

Figure 9b.- Characteristics of Cyclone supercharger at 20,000 - 21,000 rpm; tip speed, 960 - 1010 fps.

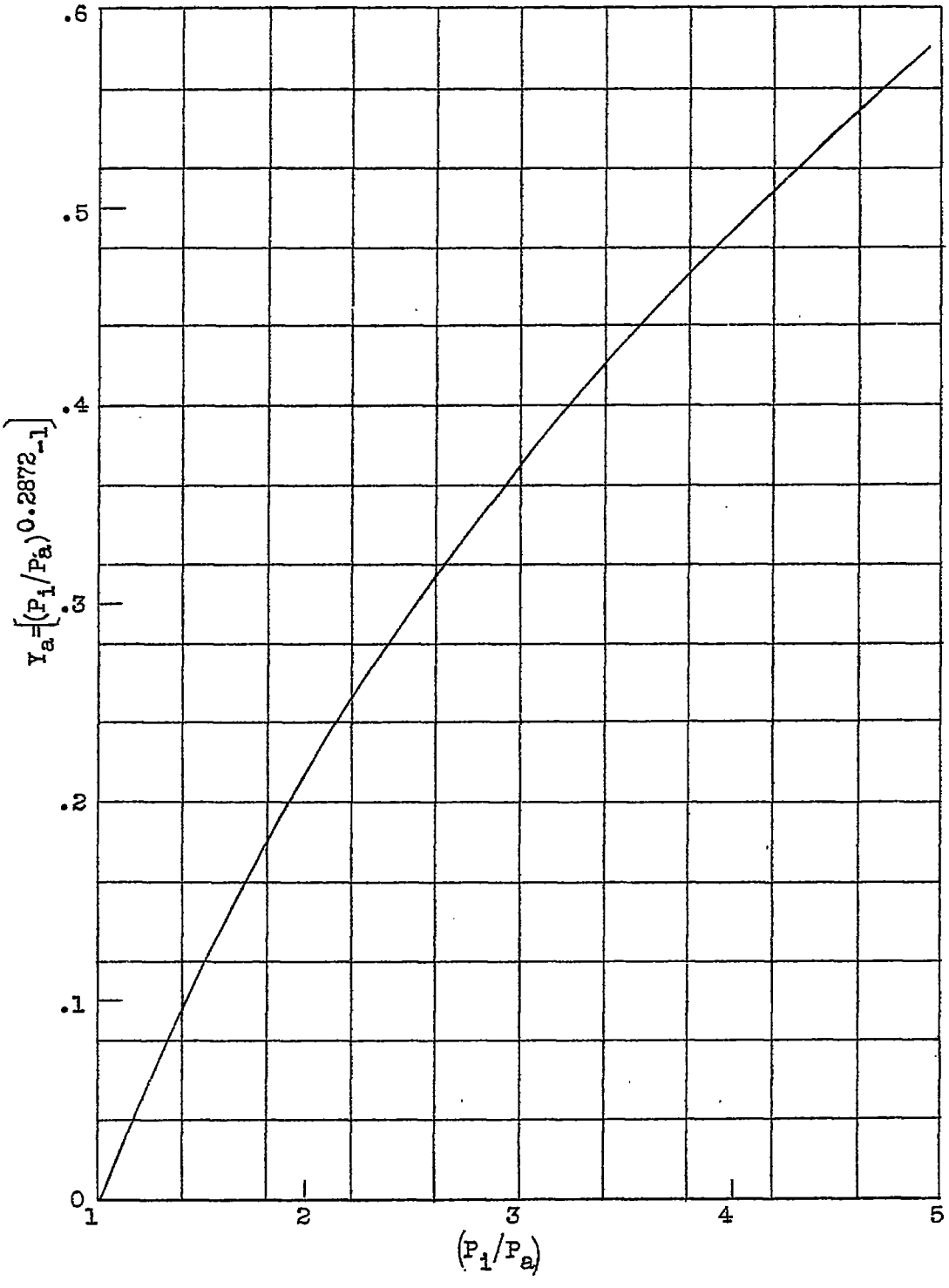

Figure 10.- Variation of Y_a with P_i/P_a.

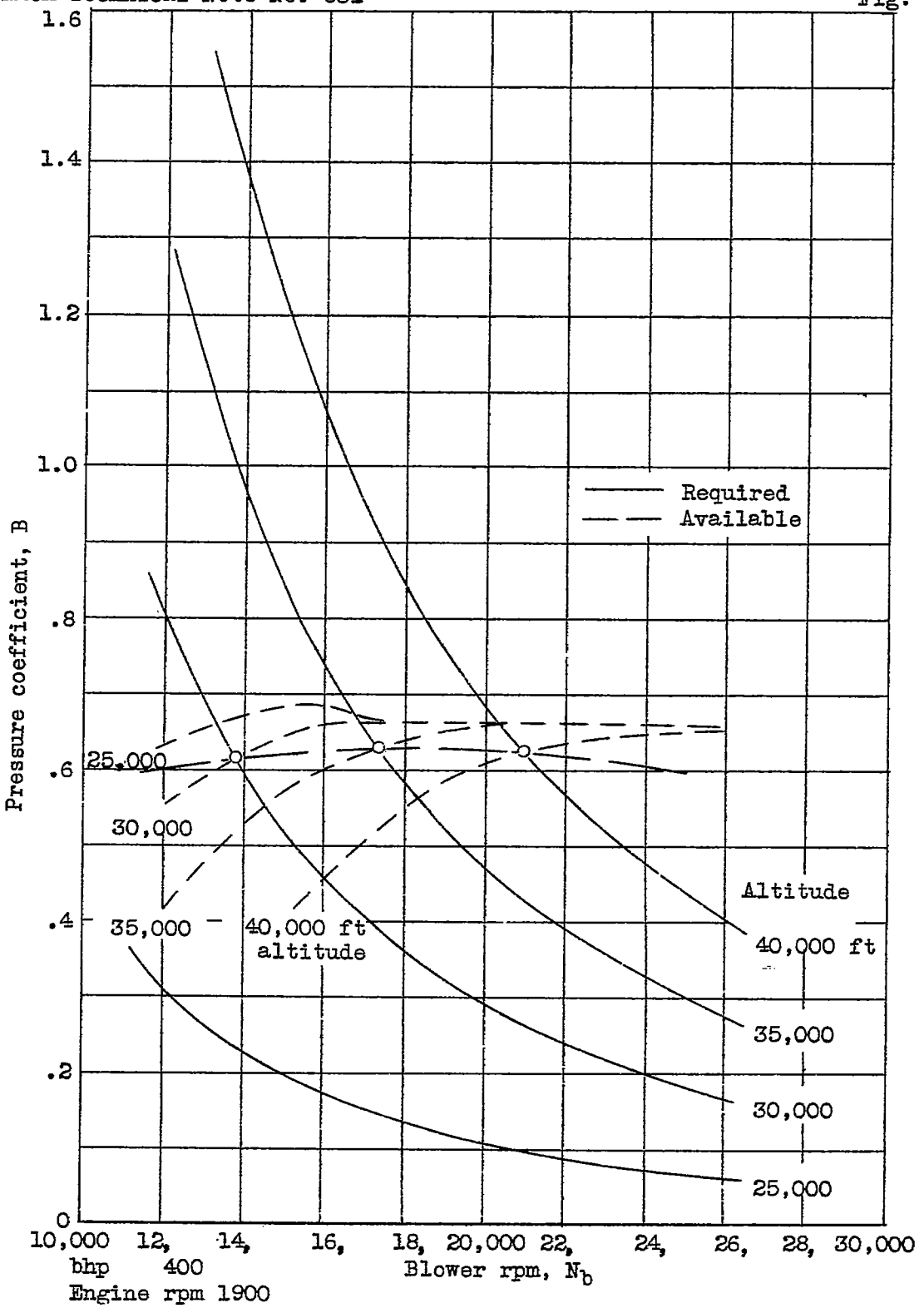

Figure 11 (a to f).- Variation of pressure coefficient with blower speed.

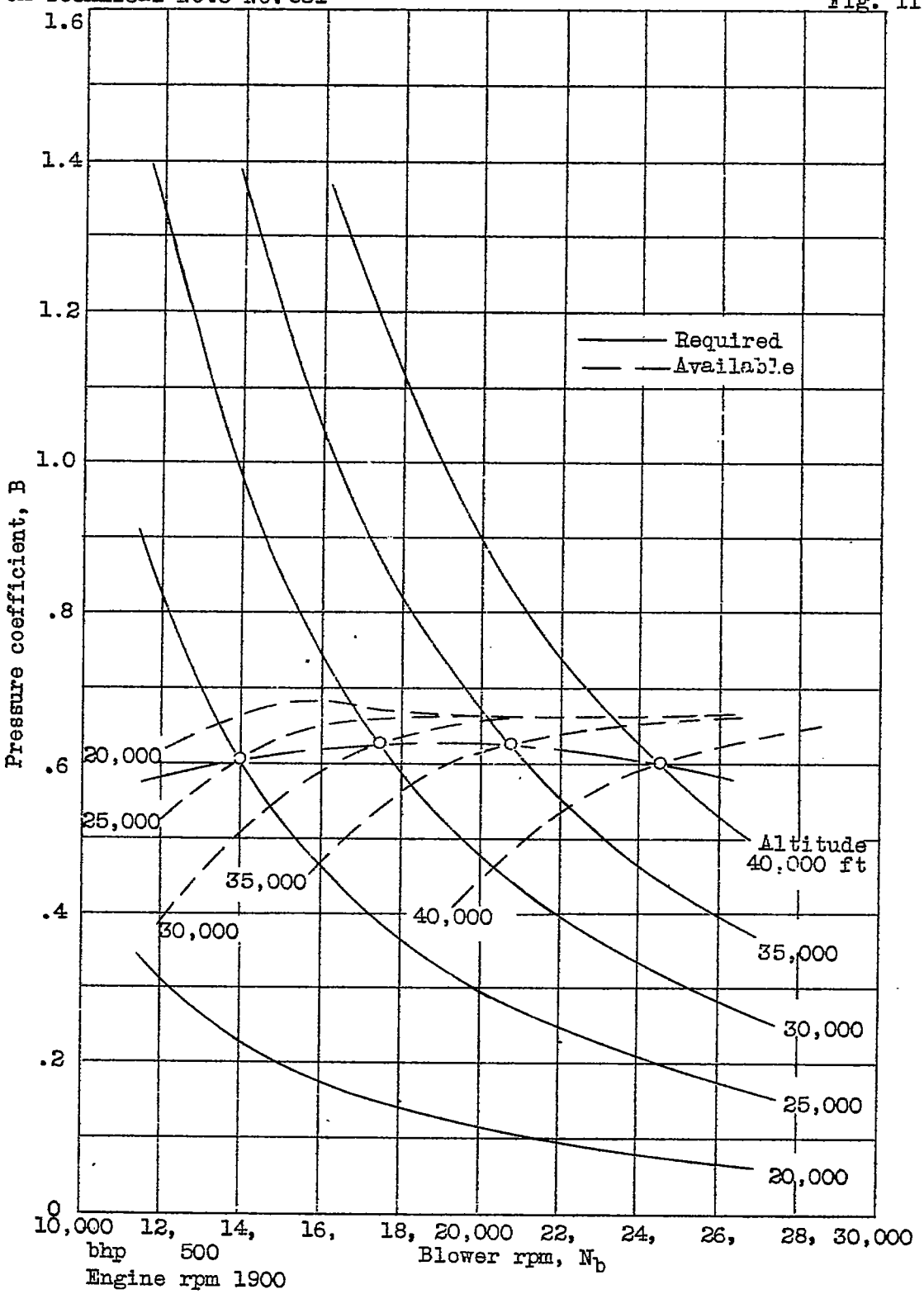
1.6
1.4
1.2
1.0
.8
.6
.4
.2
0
Pressure coefficient, B
Required
Available
20,000
25,000
30,000
35,000
40,000
Altitude
40,000 ft
35,000
30,000
25,000
20,000
10,000
12,
14,
16,
18,
20,000
22,
24,
26,
28,
30,000
bhp 500
Engine rpm 1900
Blower rpm, N_b

Figure 11 (b).

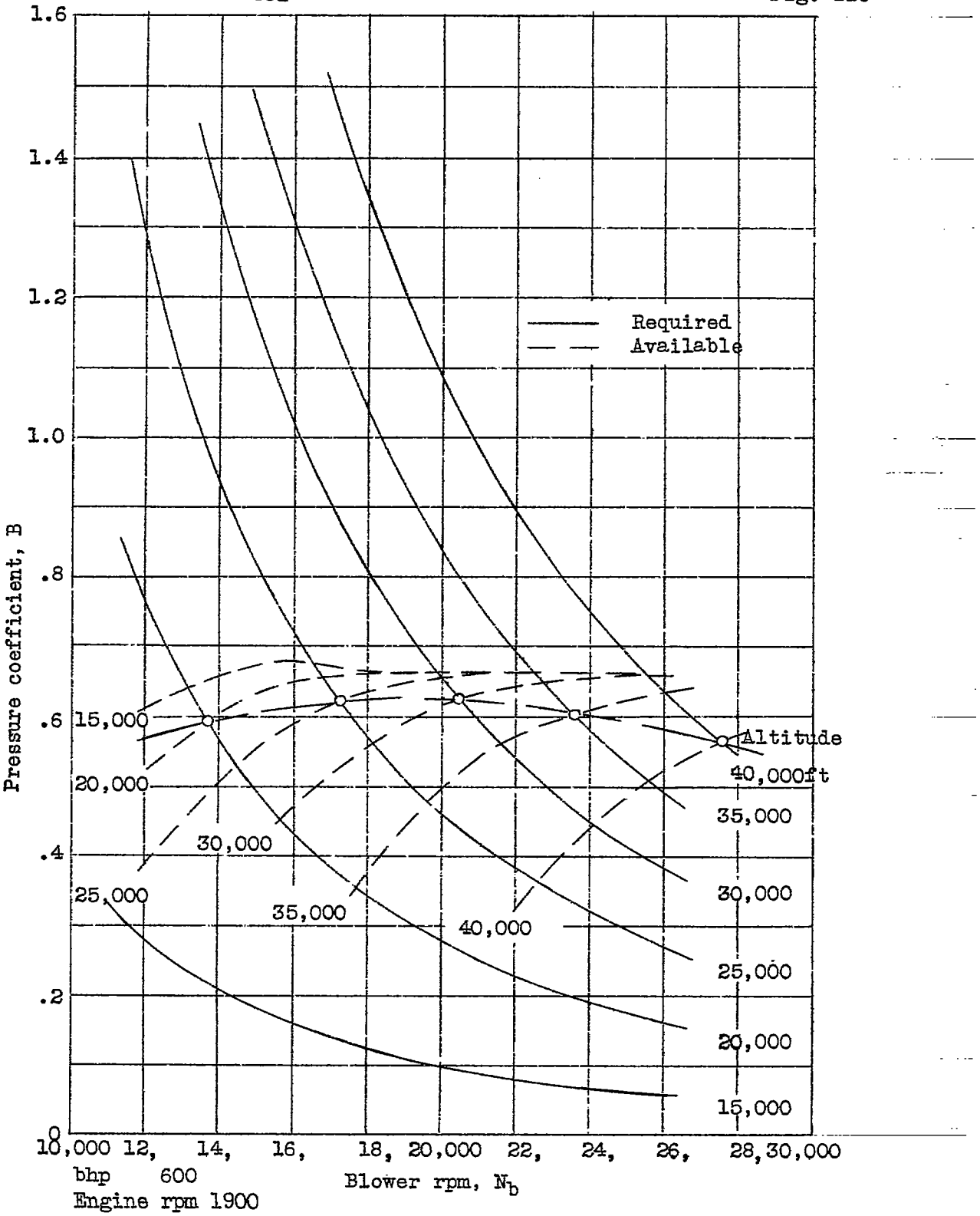
1.6
1.4
1.2
1.0
.8
.6
.4
.2
0
Pressure coefficient, B
Required
Available
15,000
20,000
25,000
30,000
35,000
40,000
Altitude
40,000ft
35,000
30,000
25,000
20,000
15,000
10,000 12, 14, 16, 18, 20,000 22, 24, 26, 28, 30,000
Blower rpm, N_b
bhp 600
Engine rpm 1900

Figure 11(c).

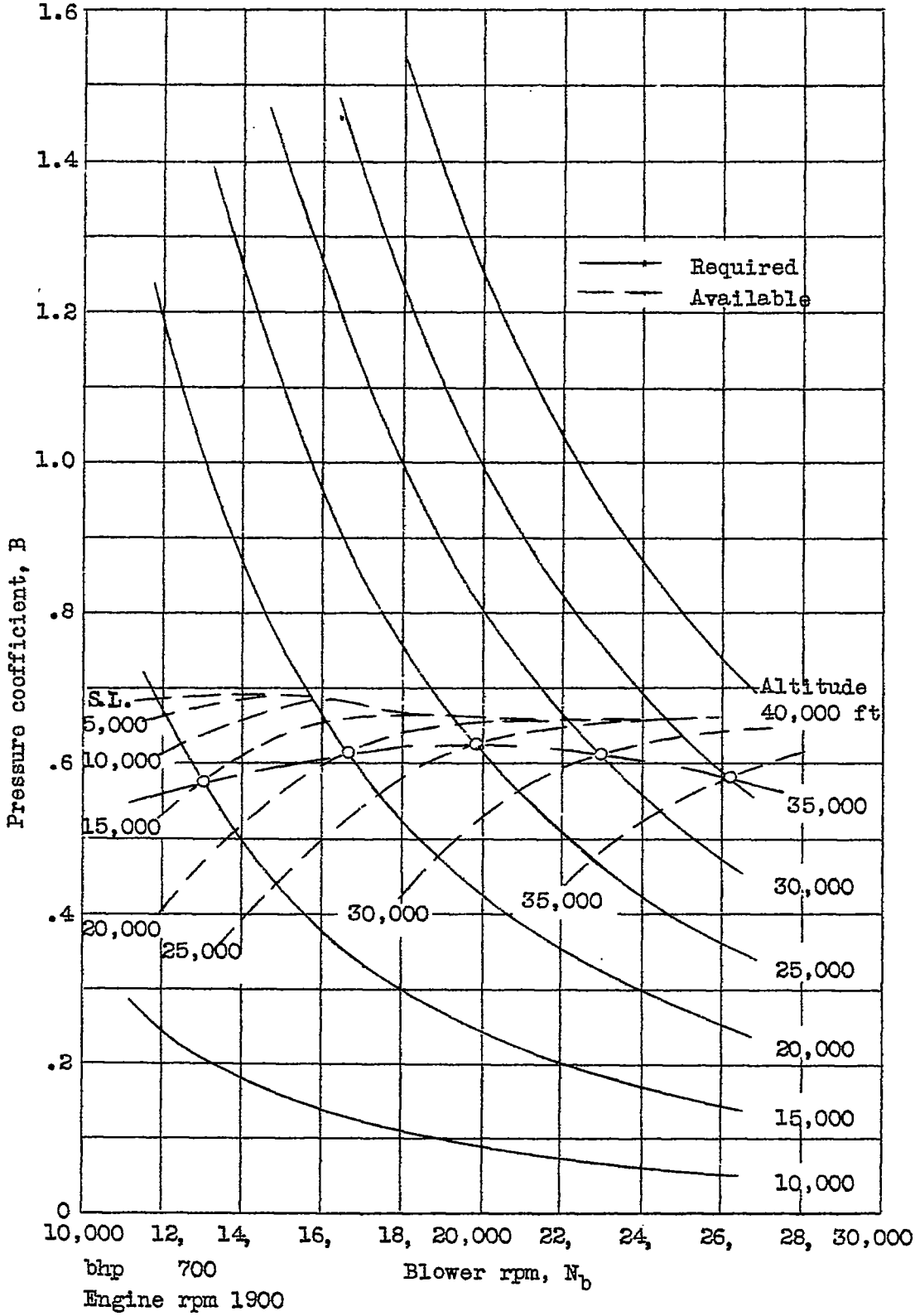
1.6
1.4
1.2
1.0
.8
.6
.4
.2
0
Pressure coefficient, B
Required
Available
Altitude
S.L.
5,000
10,000
15,000
20,000
25,000
30,000
35,000
40,000 ft
10,000
12,
14,
16,
18,
20,000
22,
24,
26,
28,
30,000
Blower rpm, N_b
bhp 700
Engine rpm 1900

Figure 11(d).

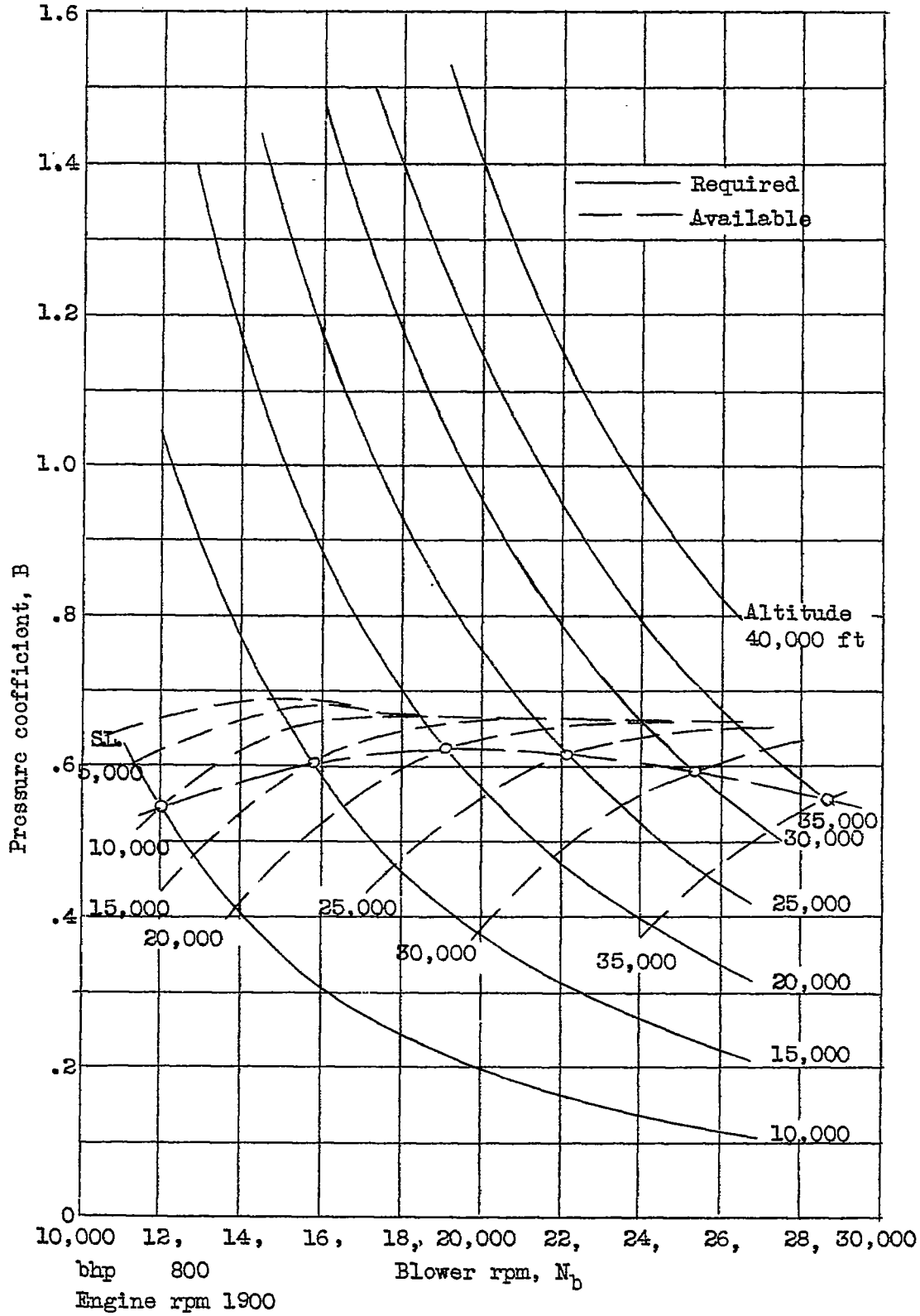
1.6
1.4
1.2
1.0
.8
.6
.4
.2
0
Pressure coefficient, B
Required
Available
Altitude
40,000 ft
35,000
30,000
25,000
20,000
15,000
10,000
S.L.
5,000
10,000
15,000
20,000
25,000
30,000
35,000
10,000 12, 14, 16, 18, 20,000 22, 24, 26, 28, 30,000
bhp 800
Engine rpm 1900
Blower rpm, N_b

Figure 11(e).

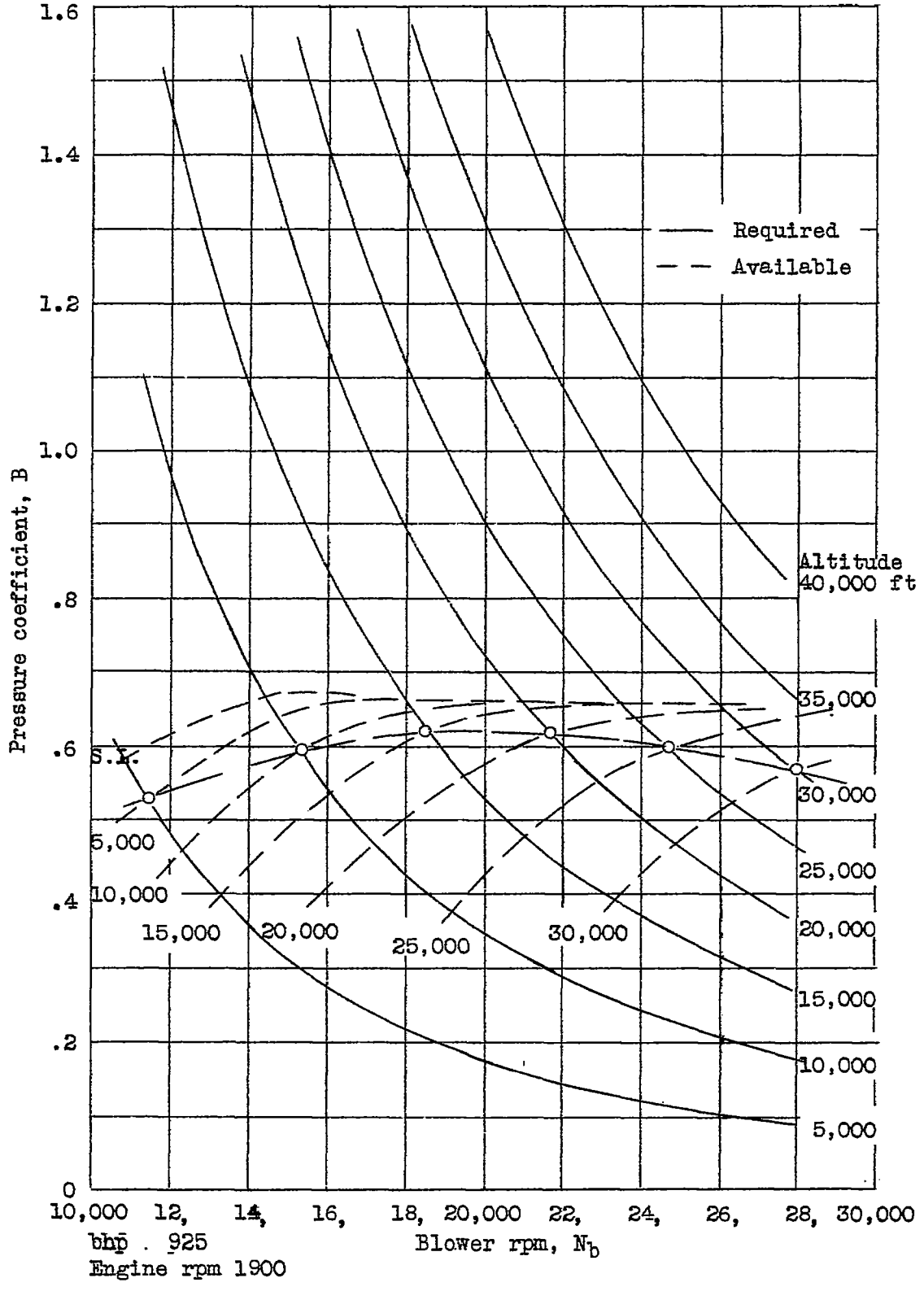
1.6
1.4
1.2
1.0
.8
.6
.4
.2
0
Pressure coefficient, B
Required
Available
Altitude
40,000 ft
35,000
30,000
25,000
20,000
15,000
10,000
5,000
S.L.
5,000
10,000
15,000
20,000
25,000
30,000
10,000
12,
14,
16,
18,
20,000
22,
24,
26,
28,
30,000
bhp . 925
Engine rpm 1900
Blower rpm, N_b

Figure 11(f).

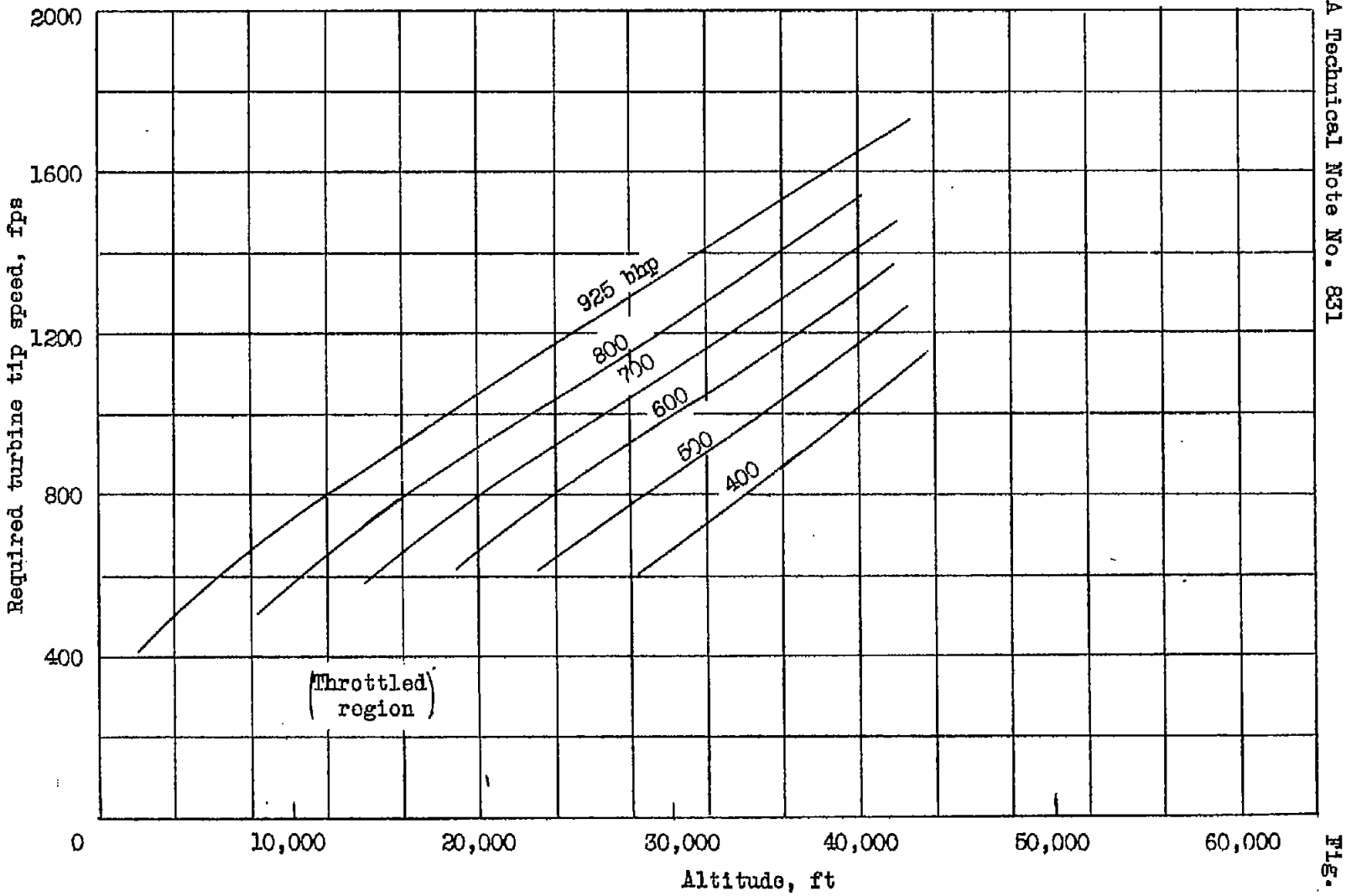

Figure 12.- Variation of turbine tip speed with altitude. Engine speed, 1900 rpm; full throttle.

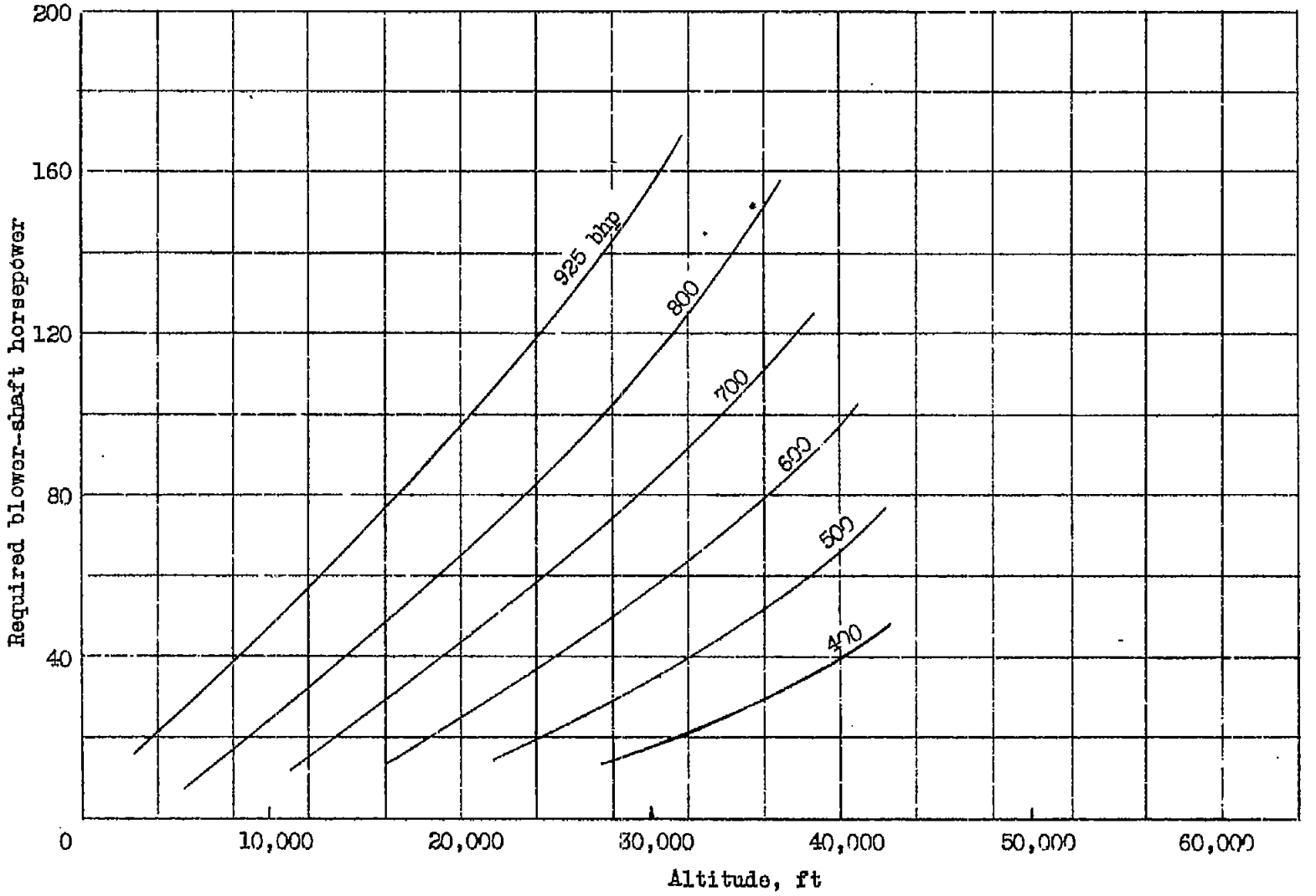

Figure 13.- Variation of blower-shaft horsepower with altitude. Engine speed, 1900 rpm; full throttle.

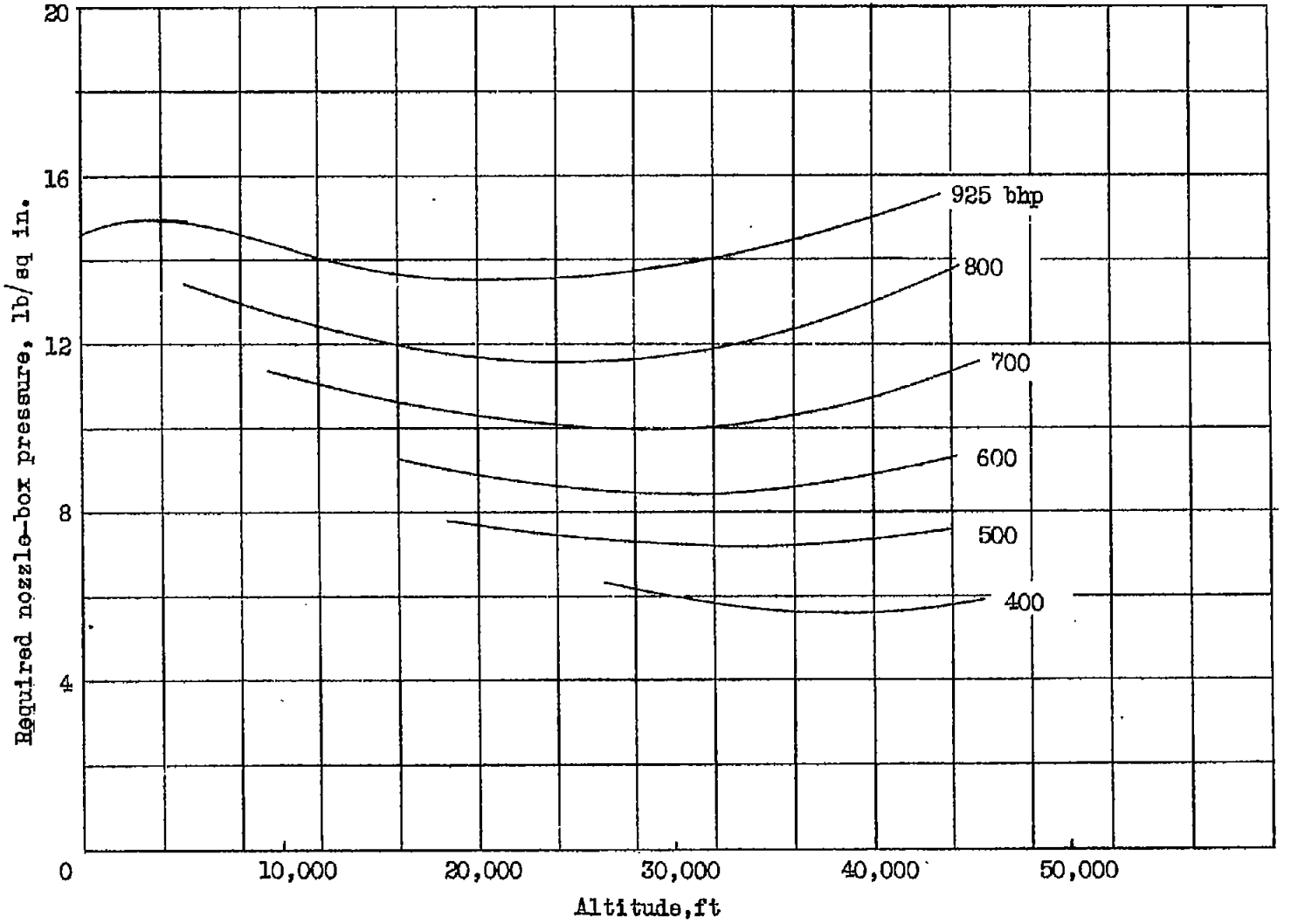

Figure 14.- Variation of nozzle-box pressure with altitude. Engine speed, 1900 rpm; full throttle.

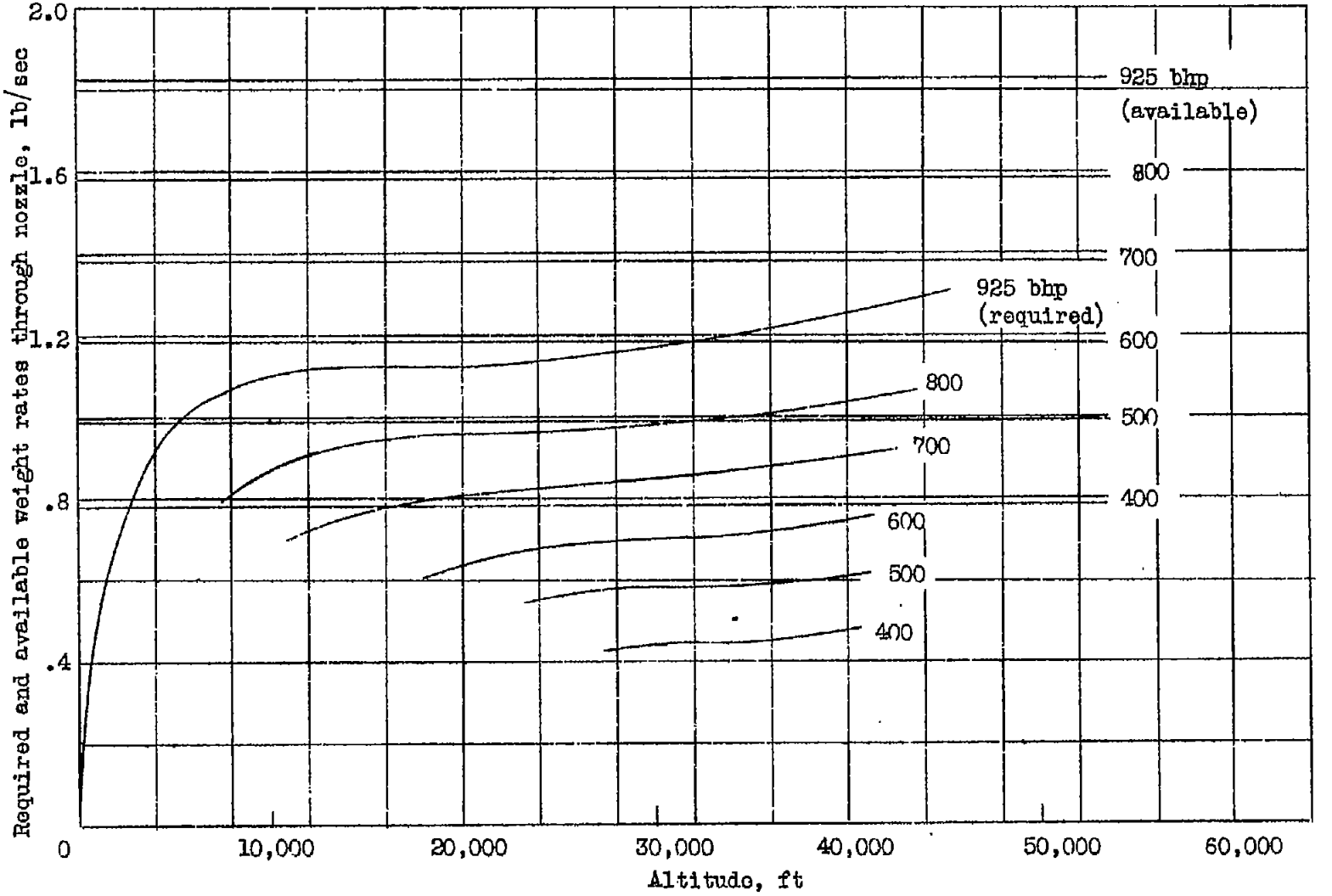

Figure 15.- Variation of rates of flow through nozzle with altitude. Engine speed, 1900 rpm; full throttle.

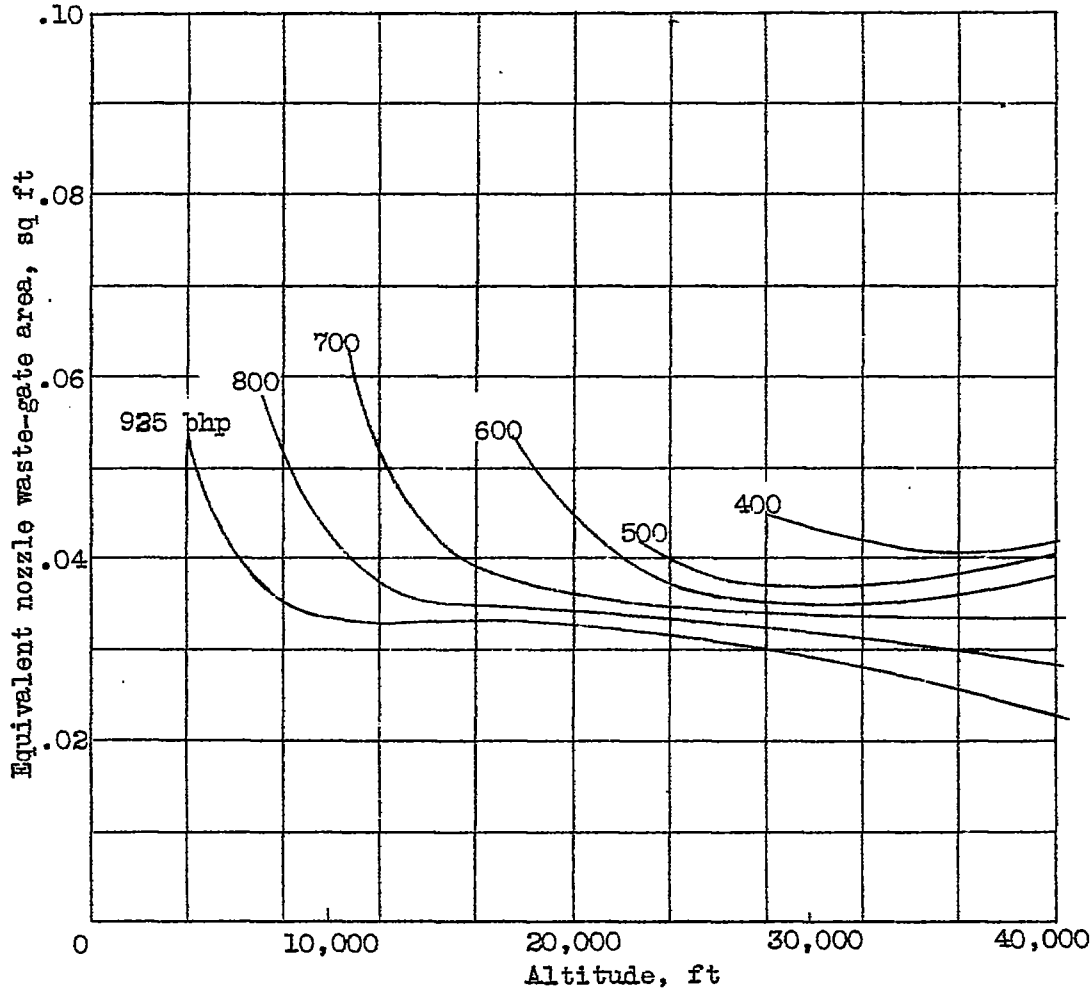

Figure 16.- Variation of waste-gate area with altitude; engine speed, 1900 rpm ; full throttle.

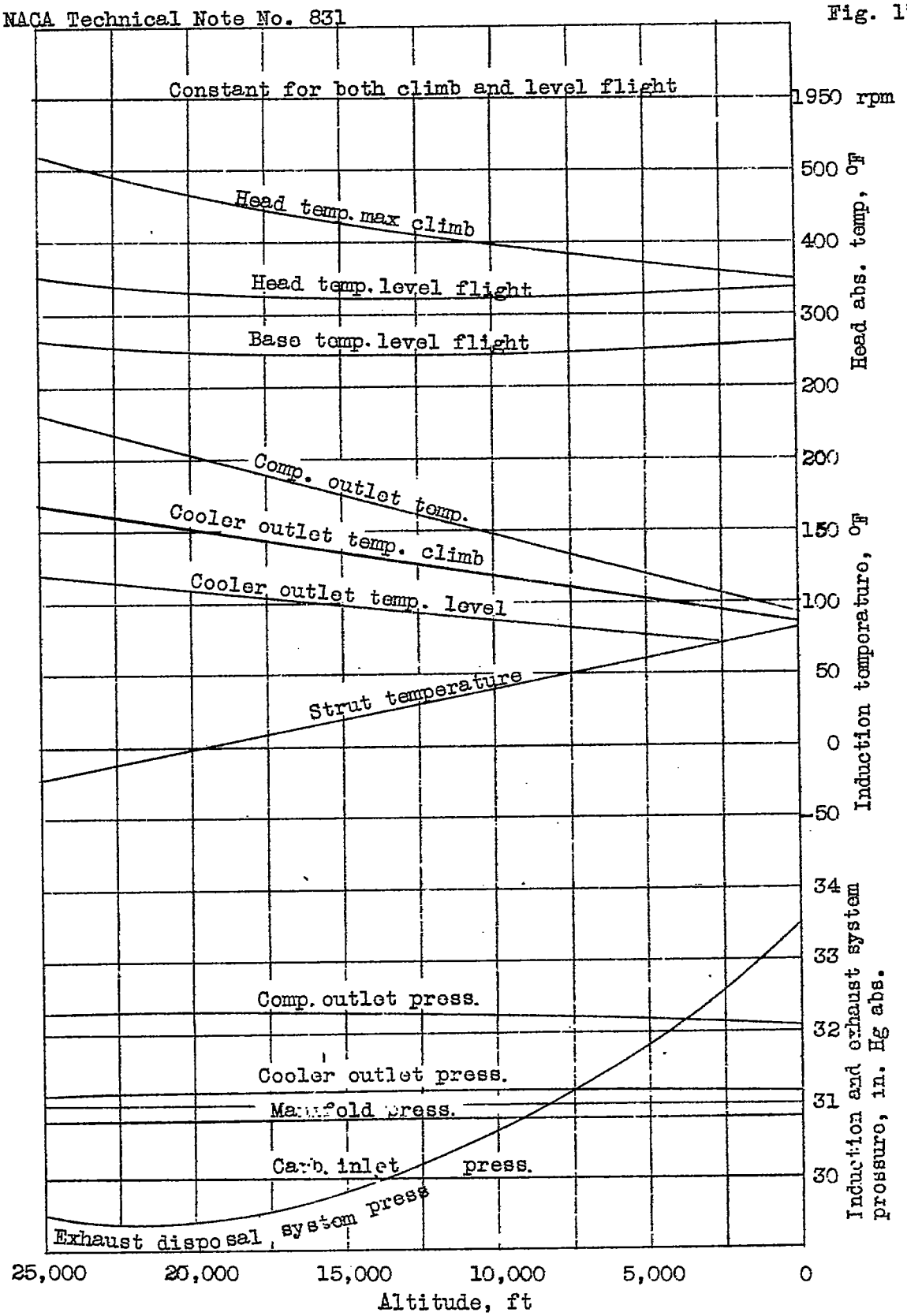

Figure 17.- Flight test of exhaust turbine-driven supercharger showing effect of properly designed disposal system (reference 4).

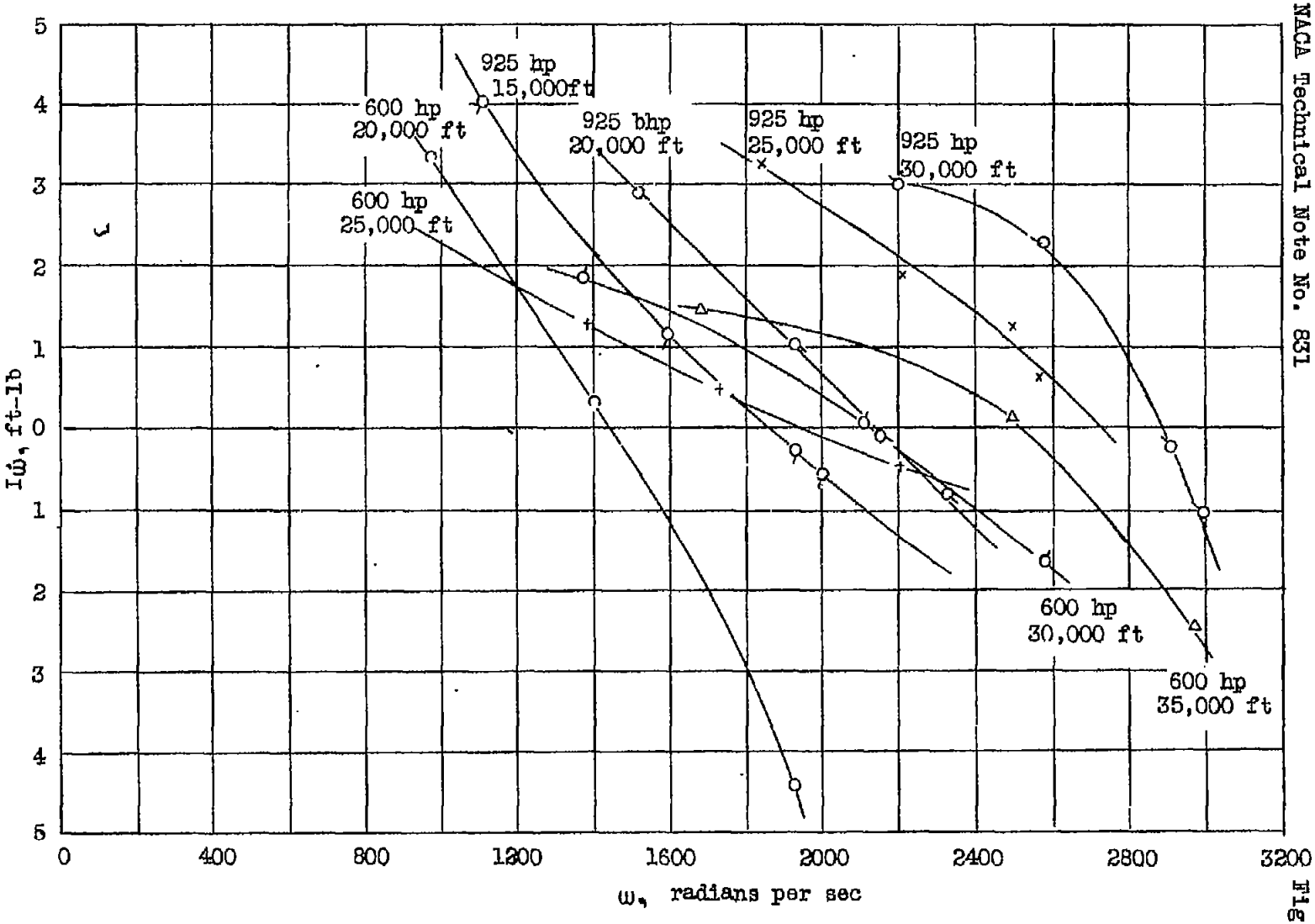

Figure 18.- Variation of $I\dot{\omega}$ with ω, $I\dot{\omega} = T_t - T_b$.